

**Weathering without inorganic CDR  
inorganic CO<sub>2</sub> removal revealed through cation tracing.  
Weathering without realizing inorganic CO<sub>2</sub> removal  
revealed though base cation monitoring.”**

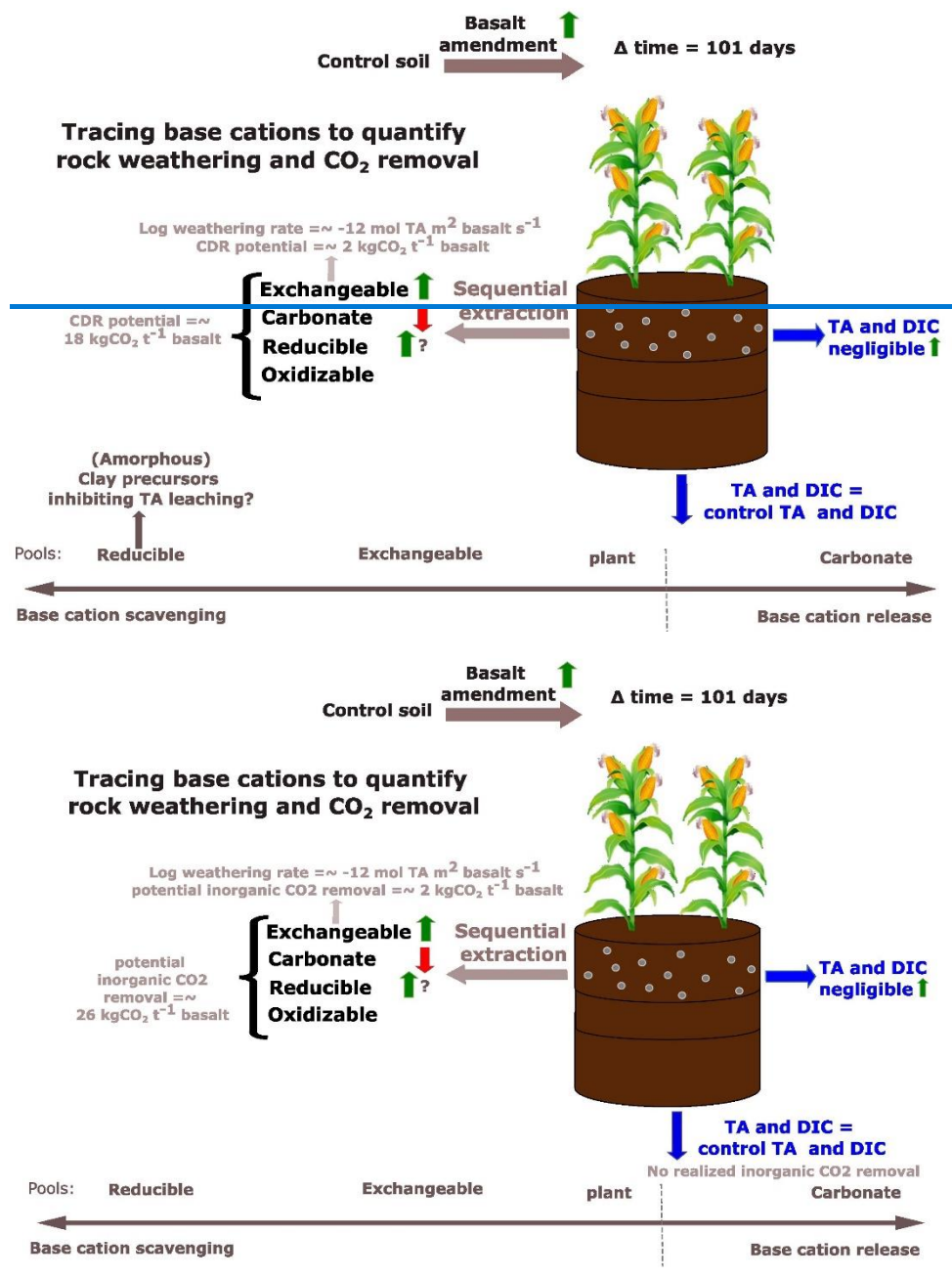
Arthur Vienne<sup>1</sup>, Patrick Frings<sup>2</sup>, Jet Rijnders<sup>1</sup>, Lucilla Boito<sup>1</sup>, Jens Hartmann<sup>3</sup>, Harun Niron<sup>1</sup>, Reinaldy P. Poetra<sup>3</sup>, Miguel Portillo Estrada<sup>1</sup>, Tom Reershemius<sup>6</sup>, Laura Steinwider<sup>1</sup>, Tim Jesper Suhrhoff<sup>4,5</sup>, Sara Vicca<sup>1</sup>

1 Biobased Sustainability Engineering (SUSTAIN), Department of Bioscience Engineering, University of Antwerp, Antwerp, Belgium  
 2 GFZ German Research Centre for Geosciences, Section Earth Surface Geochemistry, Telegrafenberg, 14473 Potsdam, Germany  
 3 Institute for Geology, Centre for Earth System Research and Sustainability (CEN), Universität Hamburg, Bundesstraße 55, 20146 Hamburg, Germany  
 4 Yale Center for Natural Carbon Capture, Yale University, New Haven, CT 06511, USA  
 5 Department of Earth and Planetary Sciences, Yale University, New Haven, CT 06511, USA  
 6 School of Natural and Environmental Sciences, Newcastle University, Newcastle upon Tyne, UK

Correspondance to: [arthur.vienne@uantwerpen.be](mailto:arthur.vienne@uantwerpen.be); [sara.vicca@uantwerpen.be](mailto:sara.vicca@uantwerpen.be)

Keywords: CDR, Enhanced weathering, MRV, sequential extractions, weathering, basalt, time lags for CDR, secondary minerals

**Graphical abstract**



20

21  
22

## Abstract

Enhanced Weathering using basalt rock dust is a scalable carbon dioxide removal (CDR) technique, but quantifying rock weathering and CDR rates poses a critical challenge. [Here, we investigated realized inorganic CO<sub>2</sub> removal \(defined as the sum of the change in dissolved inorganic C leaching and in solid inorganic C\)](#) ~~Here, we investigated inorganic CDR~~ and weathering rates by treating mesocosms planted with corn with basalt (0, 10, 30, 50, 75, 100, 150 and 200 t ha<sup>-1</sup>) and monitoring them for 101 days. ~~Surprisingly, We~~ observed no significant [realized inorganic CO<sub>2</sub> removal](#) ~~inorganic CDR~~ [inorganic CO<sub>2</sub> removal](#), as leaching of dissolved inorganic carbon did not increase, and soil carbonate content ~~even~~ declined over time.

To gain insights into the weathering processes, [we traced the fate of base cations in the soil and plants](#) ~~we analyzed the mass balance of base cations, which can be linked with anions (including HCO<sub>3</sub><sup>-</sup>) through charge balance~~. This ~~mass balance analysis~~ showed that most base cation ~~charges~~ were [retained in the topsoil reducible soil pool, typically associated with iron \(hydr\)oxides](#) ~~retained as (hydr)oxides in the reducible pool of the top soil~~, while increases in the exchangeable pool were about a factor 10 smaller. Soil base cation scavenging exceeded plant scavenging by approximately two orders of magnitude. From the base cations in all pools (soil, soil water and plants), we quantified log weathering rates of -11 mol [total alkalinity TA](#)-m<sup>-2</sup> basalt s<sup>-1</sup> ~~and a maximum CO<sub>2</sub> removal potential of the weathered base cations (i.e., CDR potential~~ [Potential inorganic CO<sub>2</sub> removal](#)) of 18 kg CO<sub>2</sub> t<sup>-1</sup> basalt. [The potential inorganic CO<sub>2</sub> removal, defined as the maximum inorganic CO<sub>2</sub> removal achievable if all weathered base cations, adsorbed by soil pools in this experiment, would leach out of the soil and be fully balanced by carbonate anions, was estimated at 26 kg CO<sub>2</sub> t<sup>-1</sup> basalt.](#)

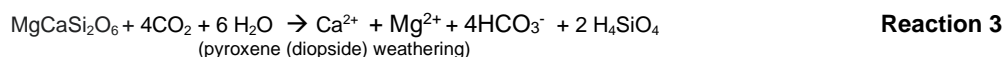
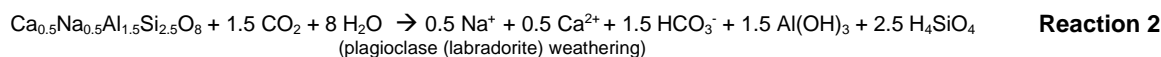
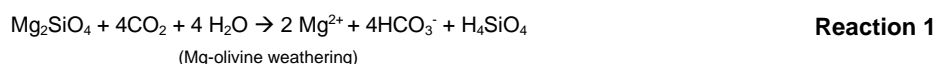
[In conclusion, despite clear weathering of basalt rock, we found no inorganic CO<sub>2</sub> removal within the timescale of this experiment. The observed increase of aluminum in association with the reducible soil fraction indicate the formation of secondary minerals. These, along with enhanced base cation exchange capacity, may contribute to long-term soil fertility and promote the stabilization of soil organic matter.](#) ~~For climate change mitigation, not only the amount of CDR potential~~ [Potential inorganic CO<sub>2</sub> removal](#) ~~is important, but also the timescale at which that CDR would be realized. Our data suggests that the lag time for realization of inorganic CDR may be larger than commonly assumed. In conclusion, we observed that inorganic CDR was not directly linked to rock weathering in the short-term. Still, the observed increases in secondary minerals and base cation exchange may provide valuable benefits for soil fertility and organic matter stabilization in the long-term.~~

## 1. Introduction

To meet the "well below 2°C warming" target established by the United Nations' Paris Agreement, Carbon Dioxide Removal (CDR) must complement conventional climate change mitigation efforts (Minx et al., 2018). One CDR technology under consideration is enhanced weathering (EW). [EW relies on accelerating natural weathering reactions of silicate minerals with water \(H<sub>2</sub>O\) and carbon dioxide \(CO<sub>2</sub>\) \(as in \*\*Reactions 1 to 3\*\*\), which increases the concentration of base cations and dissolved inorganic C \(DIC\) in water, delivering inorganic CO<sub>2</sub> removal. DIC \(the sum of aqueous \[CO<sub>2</sub>\], \[HCO<sub>3</sub><sup>-</sup>\] and \[CO<sub>3</sub><sup>2-</sup>\]\) can either be measured directly or derived through monitoring of total alkalinity \(TA\) or electrical conductivity which are less expensive to monitor and can be linked with DIC through calibration curves \(Amann & Hartmann, 2022\) \(see also \*\*Fig. S10\*\*\). This calibration is feasible because, according to the explicit conservative expression for TA in water, TA = \[HCO<sub>3</sub><sup>-</sup>\] + \[CO<sub>3</sub><sup>2-</sup>\] + \[OH<sup>-</sup>\] - \[H<sup>+</sup>\] \(Wolf-Gladrow et al., 2007\). TA can also be approximated from the sum of base cation charges, minus the sum of conservative anion charges \(e.g. chloride, sulphate, phosphate, nitrate\) \(Barker, 2013; Wolf-Gladrow et al., 2007\).](#)

63  
64  
65  
66  
67  
68  
69  
70  
71  
72

[EW relies on accelerating natural weathering reactions of silicate minerals with H<sub>2</sub>O and CO<sub>2</sub> \(as in \*\*Reactions 1 to 3\*\*\), which increases the concentration of base cations and dissolved inorganic C \(DIC\) in water\). As a proxy for DIC, total alkalinity \(TA\) is often used, which can be approximated as the sum of base cation charges \(\*\*Equation 1\*\*\) \(Amann & Hartmann, 2022; Barker, 2013; Wolf-Gladrow et al., 2007\). DIC can also precipitate as soil inorganic carbon \(SIC\) in the form of solid carbonates, thereby losing half of the initially captured CO<sub>2</sub> \(\*\*Reaction 4\*\*\) \(Haque et al., 2019\). inorganic CO<sub>2</sub> removal can be defined as the sum of changes in DIC leaching from a soil system after rock amendment plus the change in solid inorganic C \(SIC\) within the soil system after rock amendment. A robust and reliable accounting of inorganic CO<sub>2</sub> removal must thus include both monitoring of DIC leaching and SIC changes.](#)



$$\text{ATA} \approx 2 * (\Delta\text{Ca} + \Delta\text{Mg}) + \Delta\text{Na} + \Delta\text{K} \quad (1)$$

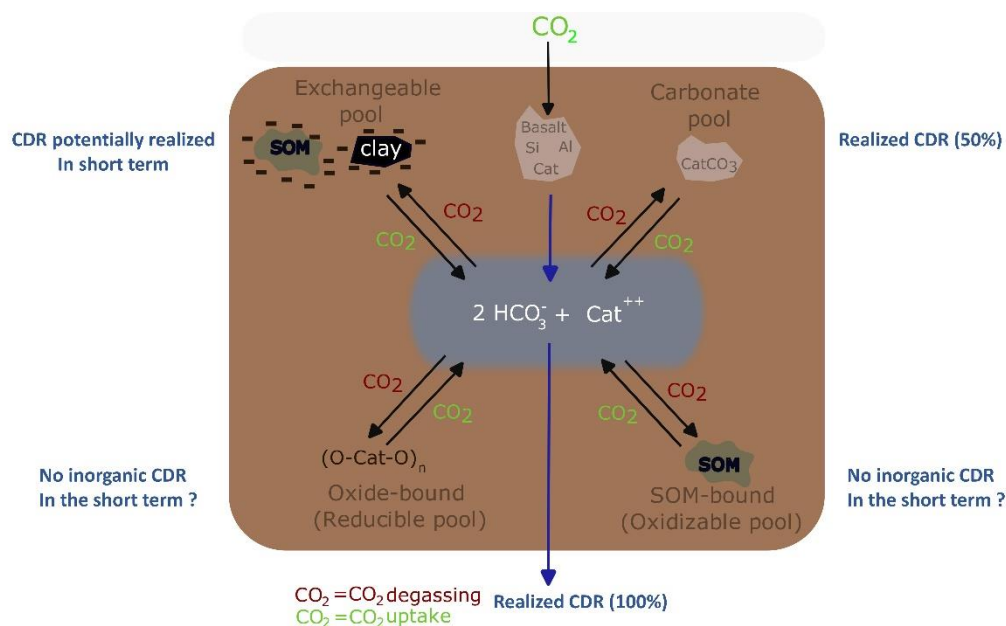
73  
74 EW is an attractive CDR technology for several reasons. First, EW may provide long-lived to permanent CO<sub>2</sub>  
75 sequestration: if fixed, DIC is transported via rivers or groundwater to oceans where it may not be released back  
76 into the atmosphere for millennia, the timescale needed for oceanic carbonate precipitation, which would release  
77 50% of the DIC input back into the atmosphere (**Reaction 4**) (Renforth & Henderson, 2017). Secondly, rock dust  
78 amendment has the potential to improve soil fertility and counters soil acidification (Swoboda et al., 2021; Van  
79 Straaten, 2006). Thirdly, unlike some other CDR technologies (such as bio-energy with carbon capture and storage  
80 (BECCS) or afforestation), EW avoids competition for land with food production (Fuss et al., 2018; Janssens et al.,  
81 2022; Smith et al., 2016). Although several rock types are considered for EW, basalt is typically used in EW field  
82 trials and has several advantages. Basalt has relatively high base cation content, particularly of Ca<sup>2+</sup> and Mg<sup>2+</sup>,  
83 which translates into a high potential for CO<sub>2</sub> removal (Renforth et al., 2019). Additionally, basalt is comprised of  
84 mafic silicate minerals such as plagioclases, pyroxene, and olivine, known for their relatively high weathering rates  
85 (Wr). Furthermore, basalt formations are abundant, widely distributed and close to major economies, making the  
86 adoption of EW using basalt scalable. Importantly, basalt is safer for agricultural application compared to ultramafic  
87 rocks like dunite due to its lower content of heavy metals such as Ni and Cr (Beerling et al., 2020).

88 [Despite the great potential of terrestrial EW and substantial attention by industry in recent years, monitoring rock](#)  
89 [weathering and CDR is challenging. Quantification of inorganic CO<sub>2</sub> removal by EW has often focussed on tracking](#)  
90 [DIC or alkalinity leaching in porewaters \(Holzer et al., 2023; McDermott et al., 2024\). However, it is also important](#)  
91 [to consider DIC in exported soil water \(leachates\) \(Larkin et al., 2022\) as changes in DIC during soil water transport](#)  
92 [are well-established. Numerous studies demonstrated that soil water movement and pH strongly govern DIC](#)  
93 [dynamics, both in soil research \(Öquist et al. 2009; Schindlbacher et al., 2019\) and in EW research \(Dietzen et al.,](#)  
94 [2018; Niron et al., 2024; Reynaert et al., 2023; Vienne et al., 2024\).](#)

95 Despite the great potential of terrestrial EW and substantial attention by industry in recent years, monitoring rock  
 96 weathering and CDR is challenging. Quantification of inorganic CDR (inorganic CO<sub>2</sub> removal) by EW has often  
 97 focussed on tracking DIC or alkalinity leaching in porewaters and drainage (Holzer et al., 2023; Larkin et al., 2022).  
 98 However, recent studies have shown that soils can greatly influence DIC leaching dynamics (Dietzen et al., 2018;  
 99 Niron et al., 2024; Reynaert et al., 2023; Vienne et al., 2024). DIC can for example precipitate as soil inorganic  
 100 carbon (SIC) in the form of solid carbonates, thereby losing half of the initially captured CO<sub>2</sub> (Reaction 4) (Haque et  
 101 al., 2019). A robust and reliable accounting of inorganic CDR (inorganic CO<sub>2</sub> removal) must thus include both  
 102 monitoring of DIC leaching and SIC changes.

103 Focusing solely on changes in DIC and SIC may however overlook other critical soil processes that impact CDR.  
 104 Besides the carbonate soil pool, other solid soil pools can also extract base cations from solution (Figure 1). These  
 105 pools (temporarily temporarily) trap base cations, preventing DIC leaching and could stabilize soil organic matter  
 106 (SOM) (Buss et al., 2024). Here, we trace the fate of cations in four different soil pools, to gain better estimates of  
 107 Wrs and CDR.

108



109

110 **Figure 1:** Schematized weathering of aluminosilicate rock and four soil pools that scavenge base cations (= alkalinity): exchangeable pool, carbonate pool, reducible pool and oxidizable pool. Because of charge balance,  
 111 uptake of base cations by these pools releases H<sup>+</sup> that can reconver HCO<sub>3</sub><sup>-</sup> (that was a priori generated from CO<sub>2</sub> through weathering) into CO<sub>2</sub>. Cat<sup>++</sup> = one divalent base cation or two monovalent base cations. In each corner,  
 112 in blue, the significance for CDR is indicated for each of the soil pools.  
 113  
 114

115 Tracing base cations in soils can be done based on the established methodology of Tessier et al. (1979) in which  
 116 cations are partitioned into four operationally defined soil pools; The exchangeable pool, the carbonate pool, the  
 117 reducible pool and the oxidizable pool. First, in the exchangeable soil pool, cations interact with negatively charged  
 118 clay or SOM surfaces. Secondly, in the carbonate pool contains carbonates such as CaCO<sub>3</sub> and the C in this pool is

119 reported as SIC. The detection of changes in SIC in basalt amended soils in short-duration experiments is typically  
120 challenging (Kelland et al., 2020; Vienne et al., 2022). Focusing on carbonate base cations may avoid typical issues  
121 with C heterogeneity and detection of relatively small SIC changes.

122 Thirdly, Tessier et al. (1979) operationally defined a reducible soil pool where base cations are associated with iron (Fe) and  
123 manganese (Mn) (hydr)oxides, and an oxidizable pool where cations are bound to SOM or sulfides. Dzombak and Morel (1990)  
124 modelled adsorption of Mg to hydrous ferric oxides (FeO(OH)), in which a surface hydroxyl group loses a proton and is  
125 replaced by a magnesium ion ( $\text{FeOOH} + \text{Mg}^{2+} \rightleftharpoons \text{FeOMg}^{+} + \text{H}^{+}$ ) and thereby decreases solute TA. In the fourth considered  
126 soil pool, the oxidizable pool, organic functional groups such as carboxylic and phenolic groups can form strong bounds with  
127 cations after deprotonation (Kalinichev et al., 2011). Cations in the oxidizable pool are expected to chemically stabilize organic  
128 matter due to cation bridging and inhibition of decomposing enzymes (Rowley et al., 2018).

129 In conclusion, base cations in these soil pools could decrease solute TA after proton release and hence degas DIC  
130 while potentially stabilizing SOM. Tessier et al. (1979) operationally defined a reducible soil pool (oxidized cations  
131 associated with Fe and Al hydroxides) and an oxidizable pool (cations that are bound to SOM). Cations in the  
132 oxidizable pool are expected to chemically stabilize organic matter due to inhibition of decomposing enzymes. Last,  
133 besides soil pools, also plants can scavenge base cations from solution. Base cations that go to the plant pool can  
134 be recycled to the aqueous phase, either through decomposition of plants in the field or through the food chain and  
135 sewage system, further complicating base cation mass balancing.

136 The undesirable side-effect of base cation scavenging (by plant/soil pools) is release of protons through charge  
137 balance, which convert negatively charged DIC ( $\text{HCO}_3^-$  and carbonate anions ( $\text{CO}_3^{2-}$ )) to  $\text{H}_2\text{CO}_3$  which is in  
138 equilibrium with gaseous  $\text{CO}_2$  ( $\text{CO}_3^{2-} + \text{H}^+ \rightarrow \text{HCO}_3^-$  and  $\text{HCO}_3^- + \text{H}^+ \rightarrow \text{H}_2\text{CO}_3 \rightleftharpoons \text{H}_2\text{O} + \text{CO}_2(\text{g})$ ). Hence, inorganic  
139  $\text{CO}_2$  removal is reversed during storage of base cations and can be realized again when base cations are released  
140 again from soil and plant pools to the aqueous phase.

141 From base cations in plant and soil pools, we can thus calculate a 'potential inorganic  $\text{CO}_2$  removal', a terminology  
142 proposed by Steinwider et al., (2025). This is a maximum quantity of Inorganic  $\text{CO}_2$  removal that can be achieved  
143 when all cations released through silicate weathering are charge-balanced by bicarbonate/carbonates and leached  
144 from soils. Base cation retention in different soil pools results in a temporal decoupling between weathering and  
145 inorganic  $\text{CO}_2$  removal. The timeframe in which the potential inorganic  $\text{CO}_2$  removal can be achieved is a major  
146 uncertainty in EW (Kanzaki et al., 2025). For weakly bound exchangeable cations, potential inorganic  $\text{CO}_2$  removal  
147 may be achieved in the relative short term of decades. Within this timeframe, because of stronger binding strengths,  
148 reducible and oxidizable base cations are more unlikely to be released and thus deliver inorganic  $\text{CO}_2$  removal.  
149 Last, inorganic  $\text{CO}_2$  removal is only achieved if the weathering agent that induced the weathering was  $\text{H}_2\text{CO}_3$  (as  
150 in Reaction 1-3). If the weathering agent is another acid (e.g. nitric acid ( $\text{HNO}_3$ ) from fertilizers), no inorganic  $\text{CO}_2$   
151 removal occurs (McDermott et al., 2024; Taylor et al., 2021).

152

153 The undesirable side effect of base cation scavenging (by plant/soil pools) is release of CO<sub>2</sub>. By charge balance,  
 154 these pools release equivalent charges of protons in return for base cations (**Figure 1**). Protons then convert  
 155 negatively charged DIC (HCO<sub>3</sub><sup>-</sup> and CO<sub>3</sub><sup>2-</sup>) to H<sub>2</sub>CO<sub>3</sub> which is in equilibrium with gaseous CO<sub>2</sub> (CO<sub>3</sub><sup>2-</sup> + H<sup>+</sup> → HCO<sub>3</sub><sup>-</sup>  
 156 and HCO<sub>3</sub><sup>-</sup> + H<sup>+</sup> → H<sub>2</sub>CO<sub>3</sub> ⇌ H<sub>2</sub>O + CO<sub>2</sub> (g)). Hence, Inorganic CDR is reversed during storage of base cations.  
 157 Hereafter, we refer to scavenged base cations as 'scavenged TA'. Once base cations are released from these pools  
 158 into the soil water, they re-sequester CO<sub>2</sub>. From scavenged TA, we can thus calculate a 'CDR potential Potential  
 159 inorganic CO2 removal'. This is a maximum quantity of inorganic CDR inorganic CO2 removal that can be achieved  
 160 after base cation leaching from soil pools.

161 Base cation retention in different soil pools results in a temporal decoupling between weathering and inorganic  
 162 CDR. The timeframe in which the CDR potential can be achieved is a major uncertainty in EW (Kanzaki et al.,  
 163 2024a). For weakly bound exchangeable cations, CDR potential may be achieved in the relative short term of  
 164 decades. Within this timeframe, because of stronger binding strengths, reducible and oxidizable base cations are  
 165 more unlikely to be released and thus deliver inorganic CDR. Last, inorganic CDR is only achieved if the weathering  
 166 agent that induced the weathering was H<sub>2</sub>CO<sub>3</sub> (as in Reaction 1-3). If the weathering agent is another acid (e.g.  
 167 HNO<sub>3</sub> from fertilizers), no inorganic CDR occurs (McDermott et al., 2024; Taylor et al., 2021).

168 In a mesocosm experiment with basalt rock powder addition, we aimed to accurately quantify the Wr and CDR  
 169 potential potential inorganic CO2 removal through quantification of base cations in the four abovementioned soil  
 170 pools, soil water and maize plants. Tracing the fate of alkalinity after its generation by the weathering of primary  
 171 minerals is key to accurately quantify basalt Wrs. Here, we make a mass balance after 101 days of experiment,  
 172 investigate the fate of base cations through exploration of sequential extractions as a monitoring, reporting and  
 173 verification (MRV) strategy and the implications for CDR.

## 174 2. Materials and Methods

### 175 2.1 experimental set-up

176 A mesocosm experiment with 30 mesocosms was constructed at the experimental site at the Drie Eiken Campus  
 177 of the University of Antwerp (Belgium). This experiment was part of a larger mesocosm experiment that aimed to  
 178 investigate heavy metal fate in silicate amended maize plants (Rijnders et al., 2024). The mesocosms (0.6 m height,  
 179 radius=0.25m) received natural rainfall and received additional water through manual irrigation (**Fig. S2**). In May  
 180 2021, the lower 40 cm of each mesocosm was filled with a slightly acidic sandy loam soil (**Table 1**).

181 **Table 1:** properties of control soil.

Control soil properties*	
<b>pH</b> (in a soil: water suspension (1:2.5))	5.66 ± 0.01
<b>Texture</b> (Sand, clay, silt %)	<b>Sandy loam</b> (61, 4, 35 %)
<b>SOC (%)**</b>	0.53 ± 0.01
<b>SIC (%)</b>	0.0031 ± 0.0002

<b>Cation exchange capacity (CEC)</b> (meq/100g)	3.03 ±0.11
<b>Base saturation (%)</b>	50 ± 5
<b>Bulk density (BD) (kg/L)</b>	1.58±0.02

182 \*Reported values represent the average ± standard error (SE) of control soil sampled at all depths after the experimental period  
183 of 101 days. \*\* Determined through loss on ignition (4h heating at 360°C and assuming a SOC/SOM ratio of 0.58 (Van Bemmelen,  
184 1890)).

185 The upper 20 cm was filled with the same soil, either unamended in the control (C) treatment (5 mesocosms), or  
186 amended with basalt (**Figure 2**). Five mesocosms received 50 ton basalt ha<sup>-1</sup>, while six others received different  
187 amounts of basalt, ranging between 10 and 200 ton/ha (**Table 2**). The basalt was mixed homogenously in the  
188 control soil using a concrete mixer. Basalt was obtained from DURABAS (<https://www.rpbl.de>. Particle size  
189 distribution (PSD) was analyzed using a mastersizer 2000 with a Hydro 2000G sample dispersion unit after  
190 removing larger particles with a 2 mm sieve. The P80 was 310.78 µm (see **Fig. S5**). The SSA was determined with  
191 a Quantachrome Autosorb iQ using the Braunauer-Emmet-Teller (BET) method. The measurement used nitrogen  
192 (N<sub>2</sub>) as adsorbate with multi-point (5 points) and isotherm (77K) settings. Samples with the same treatment were  
193 pooled in equal quantities into one sample to reduce the cost and time for analysis. All samples were degassed at  
194 300 °C with 200 minutes of soak time. High measurement quality was ensured by frequent reference (Bundesanstalt  
195 für Materialforschung und -prüfung, Germany) measurements in addition to three technical repetitions for each  
196 measurement. The BET-SSA of the basalt rock was 9.226 ± 0.08 m<sup>2</sup> g<sup>-1</sup>. X-ray diffraction (XRD) and x-ray  
197 fluorescence (XRF) analyses are provided in the supplement.

198 **Table 2:** Overview of basalt application rates. The 0 and 50 t basalt ha<sup>-1</sup> application rates were replicated in five  
199 mesocosms, while other application rates were only tested in one mesocosm. We added these replicates within  
200 individual application rates to learn about the variability between mesocosms receiving the same treatment.

Ton silicate/ha (replications)	0 (5x)	10	30	50 (5x)	75	100	150	200
-----------------------------------	-----------	----	----	------------	----	-----	-----	-----

201  
202 Basalt was mixed into the top soil on 17/5/2021. To allow leachate collection, mesocosms had a 2 cm diameter  
203 hole at the bottom. On the inside, the bottom of the pot was covered with a root exclusion mesh to prevent soil  
204 export. Glass collectors (2.3L volume) were placed under the mesocosm to collect the leachates. Leachate volumes  
205 were determined throughout the experiment and were collected for chemical analyses on seven occasions. On  
206 3/6/2021, two sweet corn seedlings (variety Tom Thumb) were planted in each the mesocosms and all pots received  
207 fertilization with NPK (96 – 10 – 79) kg ha<sup>-1</sup> by adding Ca(NO<sub>3</sub>)<sub>2</sub>, triple super phosphate (TSP, 45% P<sub>2</sub>O<sub>5</sub>) and  
208 K<sub>2</sub>SO<sub>4</sub>. The experimental duration was 101 days; plants were harvested on 26/8/2021.

209 Soil water content and temperature were recorded using Cambell Scientific sensors (CS616) that are 30 cm in  
210 length. Watering (using rain water collected from a tank) was executed manually and total water manual inputs  
211 were tracked. In addition, daily precipitation amounts (in mm) were obtained for Wilrijk (Belgium) using the open  
212 source tool ([visualcrossing.com](http://visualcrossing.com)). In the supplement, an overview of environmental conditions (rainfall, total water  
213 inputs, temperature and soil moisture) is given.



225 [Two quality control \(QC\) standards were analyzed for individual elements \(Ca, K, Mg, sodium \(Na\), silicium \(Si\) and Fe\). The](#)  
226 [mean precision of the QC standards was 0.84%, 1.12%, 0.54%, 2.79%, 1.67% and 1.30% for the respective elements. The](#)  
227 [mean accuracy for the two QC standards was 1.87%, 2.30%, 0.17%, 1.88%, 1.39% and 2.65% for Ca, K, Mg, Na, Si and Fe](#)  
228 [respectively. For TA soil water samples, mean accuracy and precision for two different QC standards were 1.51 and 1.72%](#)  
229 [respectively. The DIC measurements with FormacsHT had an accuracy and precision 1.09 and 0.23% respectively. Accuracy](#)  
230 [and precision were determined based on 12 measurements of a QC for TA \(standards: 150 and 350 mg CaCO<sub>3</sub> L<sup>-1</sup>\) and DIC](#)  
231 [\(range between 10 and 100 mg L<sup>-1</sup>\) and based on eight measurements of two different QC concentrations for each individual](#)  
232 [element.](#)

233

### 234 **2.3 Soil collection and pretreatment**

235 Top soil pH was measured on five dates. To determine top soil pH, 4 g of air dried topsoil sample was dissolved in  
236 10 mL DI water and shaken before pH measurement using a HI3220 pH/ORP meter (Hanna Instruments, Temse,  
237 Belgium). After harvesting, soils were sampled using cylindrical soil cores (100 cm<sup>3</sup>, 5 cm length x 20 cm<sup>2</sup>). Samples  
238 were taken across the depth of the mesocosm and three sampling depths were considered (0-20cm, 20-30cm, 30-  
239 50cm). The cores were dried at 70°C for 48 hours to determine water content (gH<sub>2</sub>O/g soil) and bulk density. An  
240 additional soil sample was taken at each depth, dried at 70 °C for 48 hours and used for chemical analyses.

241

242

### 243 **2.4 Sequential base cation extractions**

244 As conceptualized by Tessier et al. (1979), base cations can reside in four different soil pools: the exchangeable  
245 pool (where O-atoms on hydroxyl or carboxyl groups of clays or SOM associate with cations), the carbonate pool  
246 (cations bound in pedogenic carbonates), the reducible pool (cations bound to Al/Mn/Fe hydr(oxide)) and the  
247 oxidizable pool (cations bound to SOM). [SOM bound to cations, extracted with weak salt solutions in the](#)  
248 [exchangeable pool typically has a low turnover time \(Poeplau et al., 2018\) and is therefore thought to be more](#)  
249 [susceptible to microbial decomposition than oxidizable SOM.](#) ~~Organic matter bound to cations in these pools~~  
250 ~~typically differs in stability; SOM bound to cations in the exchangeable pool is expected to be more prone to microbial~~  
251 ~~decomposition than SOM bound in the oxidizable pool.~~

252 We adapted the original Tessier scheme by replacing 1M MgCl<sub>2</sub> with 1M NH<sub>4</sub>-acetate for extraction of the  
253 exchangeable pool, in order to be able to measure all base cations in the exchangeable pool. Likewise, Na-acetate  
254 was replaced with a mixture of acetic acid and water to be able to measure Na in the carbonate pool. We quantified  
255 SIC changes from the base cations in these acetic acid extracts (as in (Larkin et al., 2022)) (see also Equation S4).  
256 Additionally, three other SIC measurement techniques were explored to compare and the sensitivity of detecting  
257 SIC changes after amending with a range of basalt (see section S3.7).

**Table 3:** overview of sequential extraction method  
(extraction time, temperature, conditions, volume of extractants and chemical composition of extractants).

Extraction scheme	Extraction scheme Adapted Tessier et al. (1979)*
Pool 1: Exchangeable pool	10 mL 1M NH <sub>4</sub> (CH <sub>3</sub> COO) 1h, 20°C, shaker → centrifuge → sample
Pool 2: Carbonate pool	5 mL 1M acetic acid (2h, 20°C, shaker) + 4 mL H <sub>2</sub> O + 1 mL 3M NH <sub>4</sub> Acetate → sample
Pool 3: Reducible pool	20mL 0.04M NH <sub>2</sub> OH.HCl in 25% (v/v) acetic acid (pH 2) 6h, 96°C, heat bath
Pool 4: Oxidizable pool	3mL 0.02M HNO <sub>3</sub> +5mL 30%H <sub>2</sub> O <sub>2</sub> (to pH 2 with HNO <sub>3</sub> ): 2h, 85°C, heat bath +3mL 30%H <sub>2</sub> O <sub>2</sub> (to pH 2 with HNO <sub>3</sub> ) 3h, 85°C, heat bath +5mL 3.2M NH <sub>4</sub> (CH <sub>3</sub> COO) (in 20 vol%HNO <sub>3</sub> ) +4 mL H <sub>2</sub> O 0.5h, 20°C, shaker

Prior to extractions, approximately 1g of soil was air dried. We also conducted the extractions for the pure basalt that was initially added to the mesocosms to be able to correct for the cations that were initially already present as exchangeable, carbonate, reducible and oxidizable pool cations. After each extraction, samples were centrifuged for 2 minutes at 2000 rpm, supernatants were collected for analysis. The remaining soil pellet after centrifugation was washed with 10 mL of demineralized water before the following step. Relevant elements (K, Na, Mg, Ca, Al, Fe and Si) were measured in each pool using ICP-OES (iCAP 6300 duo, Thermo Scientific) for each pool. Si was only assessed in the reducible pool and in the oxidizable pool to investigate whether Si forms amorphous oxides or allophane-like compounds or binds with organic matter. Al carbonates were not quantified here as naturally these carbonates are not commonly formed (Takaya et al., 2019).

## 2.5 Plant responses

On 26/8/2021 (101 days after basalt amendment in soils), the aboveground biomass was harvested and dried for 48h at 70 °C to determine dry weight. Plant material was ground with an ultra-centrifugal mill (Model ZM 200, Retsch GmbH, Haan, Germany). Base cations (Ca, Mg and K) were measured through ICP-OES (iCAP 6300 duo, Thermo Scientific) in aboveground biomass to calculate plant base cation stocks. Base cations were measured separately in all aboveground biomass parts: stems, leaves, flowers and corn ears.

## 2.6 Calculation of $W_r$ and **CDR-potential** Potential inorganic CO<sub>2</sub> removal

We use the delta ( $\Delta$ ) symbol to denote the difference relative to unamended control soil. Accordingly, we quantify  $\Delta TA$  (the change in total alkalinity in the basalt-amended soil relative to the control) based on the difference in base cation concentrations between amended and unamended soils. As basalt only contains cations and no conservative anions, we assume that  $\Delta TA$  can be quantified from the change in base cation charges (Equation 1).

~~We use a delta ( $\Delta$ ) to refer to differences relative to unamended control soil throughout this work.~~

$$\Delta TA \approx 2 * (\Delta Ca + \Delta Mg) + \Delta Na + \Delta K - \Delta \text{conservative anions}$$

*with  $\Delta$ conservative anions = 0*

(1)

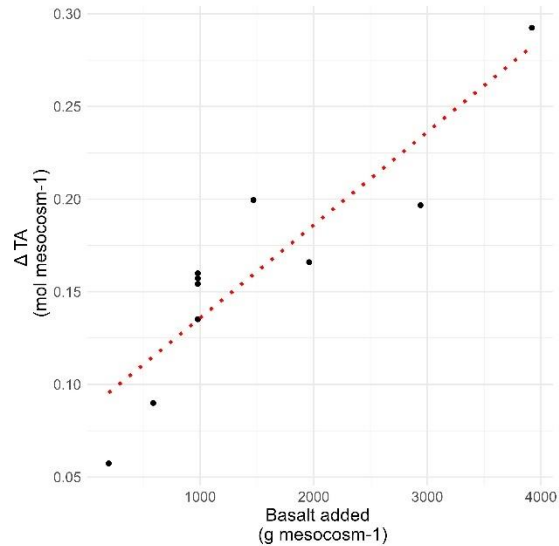
292 The  $W_r$  corresponds to the rate of rock dissolution. The  $W_r$  can be expressed per element or as moles of alkalinity  
 293 equivalents (i.e. the sum of base cation charges (**Equation 1**) per amount of rock surface area per unit of time (in  
 294  $\text{mol m}^{-2}\text{rock s}^{-1}$ ). In addition, we calculate a 'potential inorganic CO<sub>2</sub> removal'. We use the same definition for  
 295 potential inorganic CO<sub>2</sub> removal as in Steinwider et al. (2025). A 'potential inorganic CO<sub>2</sub> removal' can be defined  
 296 as the maximum amount of inorganic CO<sub>2</sub> that could be removed if all experimentally determined, weathered, soil-  
 297 retained base cations were to leach from the soil and be completely balanced by carbonate anions. Potential  
 298 inorganic CO<sub>2</sub> removal was previously 'CDR potential' by Niron et al. (2024)). The concept of CDR potential was  
 299 first introduced by Phil Renforth (2019) to describe the maximum inorganic CO<sub>2</sub> removal achievable if all base  
 300 cations within a rock were to completely weather. More recently, Beerling et al., (2024) quantified base cation losses  
 301 from topsoils using an immobile/mobile tracer approach (see Section 4.2), from which they also derived a measure  
 302 of CDR potential. To maintain conceptual clarity, we avoid using the term CDR potential for purposes other than its  
 303 original definition by Renforth (2019). When the term is employed, its meaning should always be explicitly stated.  
 304 ~~We can use the TA increase in the system to calculate a 'CDR potential' (previously named inorganic CDR~~  
 305 ~~equivalents by Vienne et al. (2023)). We define the CDR potential~~Potential inorganic CO<sub>2</sub> removal as the maximum  
 306 ~~inorganic CDR~~inorganic CO<sub>2</sub> removal that would be achieved if all base cations released during weathering that  
 307 ~~are currently retained in plants and soils are exported to the ocean as alkalinity (**Equation 10**).~~

308 To calculate the  $W_r$  (from all base cation increases relative to controls in plants, extracted soil fractions and soil  
 309 water leachates), we sum changes in TA in the following pools: exported soil water (leachates), plants and soil  
 310 pools. We can express changes in the cation pool of each reservoir as the equivalent  $W_r$  required to supply the  
 311 cations ( $W_{r\text{leachate}}$ ,  $W_{r\text{plant}}$  and  $W_{r\text{soil}}$ ) (**Equation 2**). Conventionally  $W_r$ s are expressed using a logarithmic scale as  
 312 absolute values can vary strongly. ~~We use a delta ( $\Delta$ ) to refer to differences relative to unamended control soil~~  
 313 ~~throughout this work.~~

$$314 \quad \text{Log } W_r \left[ \frac{\Delta \text{mol TA}}{\text{m}^2 \text{rock.s}} \right] = \text{Log} \left( \frac{\Delta \text{mol TA}_{\text{soil}} + \Delta \text{mol TA}_{\text{plant}} + \Delta \text{mol TA}_{\text{leachate}}}{\text{m}^2 \text{rock.s}} \right) \quad (2)$$

315  
 316 We used a gradient of rock applications, where we calculated the slope of the molar change in base cation charges  
 317 (expressed as an equivalent "alkalinity" change if these base cations were dissolved in water) with higher rock  
 318 amendment (TA slope) (**Figure 3**). We compared logarithmic and linear regression and selected the linear  
 319 regression approach, as both approaches had comparable  $R^2$  and Akaike Information Criterion (AIC) values AIC  
 320 values and linear slopes ease further data processing (**Fig. S23 and Table S5**). We opted for the linear regression  
 321 approach to simplify subsequent calculations. To make our gradient approach more robust, we also calculated the  
 322 log  $W_r$  for individual application rates in **Fig. S13**.

323



324

325 **Figure 3:** Illustration of the calculation of TA slope: The alkalinity scavenging by a given pool was plotted in function  
 326 of the applied basalt, after which the slope was used to quantify a  $W_r$ . This figure is an example regression with  
 327 data for the top soil exchangeable pool. All regressions can be found in **Fig. S223**.

328 Then we converted units of the alkalinity slope for increasing rock application (TA slope) per unit of rock mass to  
 329 moles of alkalinity per rock surface area and per time (**Equation 3**). Equation 3 was used to calculate  $\Delta\text{mol TA m}^{-2}$   
 330  $\text{rock s}^{-1}$  of base cations in leachates, plants and of every measured soil pool at every soil depth.

331

$$\frac{\Delta\text{mol TA}}{\text{m}^2 \text{ rock. s}} = \frac{\text{Scavenged alkalinity (= TA slope)} \left[ \frac{\Delta\text{mol TA}}{\text{g rock}} \right]}{\text{Experimental duration [s]} * \text{SSA}_{\text{silicate}} \left[ \frac{\text{m}^2 \text{ surface area}}{\text{g rock}} \right]} \quad (3)$$

332  $\Delta\text{mol TA m}^{-2} \text{ rock s}^{-1}$  was thus quantified per pool, based on the change in base cations in the basalt treatment  
 333 compared to the control treatment. For plants, we calculate TA slope through regression of harvested base cations  
 334 with basalt application. Harvested base cations were calculated as the product of harvested aboveground biomass  
 335 and their base cation content. Charge contributions of Na were not included; Na was not quantified at the time of  
 336 plant biomass elemental analysis, which may lead to an underestimation of the alkalinity equivalent increase in the  
 337 plant pool. However, given that base cation charges in the plant pool were about two orders of magnitude smaller  
 338 than in the soil pool, we expect the effect of this omission to be limited. In addition, maize plants aim to actively  
 339 increase their K/Na ratio which avoids salt stress, the K content of maize shoots is typically about 2 orders of  
 340 magnitude larger than Na (Gao et al., 2016; Suarez & Grieve, 1988). For leachates, TA slope was calculated as  
 341 the product of mean cumulative leachate volume and mean leachate TA concentration for each application rate and  
 342 regressing them with the applied basalt as dependent variable.

343 Finally, the  $W_r$  attributable to the change in cation content of the soil pools ( $W_{r\text{soil}}$ ) was calculated by summing the  
 344  $W_{r\text{soil\_layer\_k\_pool\_j}}$  for each pool and depth (**Equation 4**). Here, we sum changes in all pools of the topsoil (0-20 cm)  
 345 and lower depths (20-30 cm and 30-50 cm) to obtain an aggregate value for  $W_{r\text{soil}}$ . With

346  $Wr_{soil,layer k, fraction j}$  calculated as in **Equation 4** (with  $k$  = the number of depths and  $j$  = the number of considered  
 347 soil pools). TA slope at every depth and soil pool was calculated as in **Equation 5**.

$$348 \quad Wr_{soil} = \sum_{k=1}^3 \sum_{j=1}^4 Wr_{soil,layer k, pool j} \quad (4)$$

$$349 \quad \frac{\text{scavenged TA (TA slope)} \left[ \frac{\Delta \text{mol}}{\text{g rock}} \right]}{\frac{\frac{\mu \text{mol TA}}{\text{g dry Soil}} (\text{Amended Soil}) - \frac{\mu \text{mol TA}}{\text{g dry Soil}} (\text{control Soil})}{\text{Application rate (Amended soil)} [\text{g rock m}^{-2} \text{ ground area}] * 1000} * \text{Bulk Density} \left[ \frac{\text{kg dry Soil}}{\text{m}^3 \text{ soil}} \right] * \text{thickness soil layer [m]}} \quad (5)$$

350 TA per gram of dry soil mixture can be calculated for each mesocosm by summing the charges from each base  
 351 cation (**Equation 6**).

$$352 \quad \frac{\mu \text{mol TA}}{\text{g dry Soil}} = \sum_{j=1}^4 \left( \frac{\frac{\mu \text{g Ca}_{pool j}}{\text{g dry soil}}}{40.078 \frac{\text{gCa}}{\text{molCa}}} + \frac{\frac{\mu \text{g Mg}_{pool j}}{\text{g dry soil}}}{24.305 \frac{\text{gMg}}{\text{molMg}}} \right) * \frac{2 \text{mol TA}}{\text{mol cat}^{++}} + \left( \frac{\frac{\mu \text{g Na}_{pool j}}{\text{g dry soil}}}{22.990 \frac{\text{gNa}}{\text{molNa}}} + \frac{\frac{\mu \text{g K}_{pool j}}{\text{g dry soil}}}{39.098 \frac{\text{gK}}{\text{molK}}} \right) * \frac{1 \text{mol TA}}{\text{mol cat}^+} \quad (6)$$

353 [These individual base cations \(e.g. Ca in pool j\) are calculated from the difference of cations weathered during the](#)  
 354 [weathering operation minus the cations initially present in that fraction in the applied feedstock \(Power et al., 2025\)](#)  
 355 [\(Equation 7\). These individual base cations \(e.g. Ca in pool j\) are calculated from the difference of cations](#)  
 356 [weathered during the weathering operation minus the cations that were already weathered initially in the feedstock](#)  
 357 [rock \(Equation 7\).](#) For example, some cations can already exchange on the surface or edges of the applied  
 358 minerals, so that these cannot be counted as weathered, they will however contribute to CDR once leached.

359 To calculate in-situ  $Wr$ , it is thus necessary to correct for the cations that had already been weathered from primary  
 360 minerals at the time of silicate amendment. This correction is currently not being done in EW literature yet. As basalt  
 361 is only added to the top soil and not deeper, this correction is only done for the 0-20 cm soil layer here.

$$362 \quad \frac{\mu \text{g element}_{i, pool j}}{\text{g dry soil}} = \left( \frac{\mu \text{g element}_{i, pool j}}{\text{g dry soil}} \right)_{\text{Post weathering, soil mixture}} - \left( \frac{\mu \text{g element}_{i, pool j}}{\text{g dry soil}} \right)_{\text{added with feedstock initially}} \quad (7)$$

363 The mass of a specific element (i) in each of the four (j) soil pools (in  $\mu \text{g element/g soil}$ ) is calculated using **Equation**  
 364 **8**.

$$365 \quad \left( \frac{\mu \text{g element}_{i, pool j}}{\text{g dry soil}} \right)_{\text{Post weathering, soil mixture}} = \frac{\text{concentration element}_i \text{ in pool}_j \left[ \frac{\text{mg}}{\text{L}} \right] * \text{Volume extract}_j [\text{mL}]}{\text{mass of solid extracted [g]}} \quad (8)$$

366 The initial addition of element i to pool j is calculated as in **Equation 9**.

$$367 \quad \left( \frac{\mu \text{g element}_{i, pool j}}{\text{g dry soil}} \right)_{\text{added with feedstock initially}} = \frac{\mu \text{g element}_i \text{ pool}_j}{\text{g silicate}} * \frac{\text{Application rate} \left[ \frac{\text{g silicate}}{\text{m}^2} \right]}{\text{Bulk density} \left[ \text{g dry soil} \frac{\text{m}^3}{\text{m}^3} \right] * \text{depth of soil amendment [m]}} \quad (9)$$

368 According to the charge balance (**Reaction 1-3**) during mineral dissolution, 1 mol  $\text{HCO}_3^-$   $\text{mol}^{-1}$  TA is generated (and  
 369 thus 1 mol of  $\text{CO}_2$  is sequestered). We define a factor  $\eta$ , that is equal to the ratio of  $\text{HCO}_3^-$  per mol of generated  
 370 TA. According to charge balance,  $\eta=1$ . A more conservative approach is to assume that all this generated alkalinity

371 will be exported to the ocean, after which chemical equilibrium degasses a portion of the alkalinity ( $\eta = 0.7 \text{ mol CO}_2$   
 372  $\text{mol}^{-1} \text{ TA}$ , assumed for oceans) (Renforth et al., 2012; Renforth et al., 2019; Renforth & Henderson, 2017).  
 373 According to Renforth et al. (2019), the ocean alkalization efficiency  $\eta$  ranged between 0.7 and 0.85. This  $\eta$   
 374 parameter is relatively uncertain given that model studies indicate that  $\eta$  can range between 0.65 and 0.8  $\text{mol CO}_2$   
 375  $\text{mol TA}^{-1}$  (see section S6 in the supplement of (Katarzyna et al., 2024)). Alternatively, we can assume that all base  
 376 cations will form solid carbonates in soils or rivers. In this case  $\eta=0.5 \text{ mol CO}_2/\text{mol TA}$  (**Reaction 4**). In Table 4,  
 377 we calculated potential inorganic CO<sub>2</sub> removals assuming conservative values of  $\eta=0.5$  (carbonate precipitation  
 378 scenario) and  $\eta=1$  (the highest possible  $\eta$  without any downstream DIC losses).

379 ~~In Table 4, we calculated CDR potentials assuming conservative values of  $\eta=0.5$  (carbonate precipitation scenario)~~  
 380 ~~and the most optimistic value  $\eta=1$ .~~

381 While calculating  $W_r$ , cations added with the rock feedstock that were already weathered were subtracted as in  
 382 Equation 7, yet these cations are not subtracted to calculate the potential inorganic CO<sub>2</sub> removal as base cations  
 383 in weathered fractions of the rock feedstock can also leach to soil water whereby HCO<sub>3</sub><sup>-</sup> is generated. Last, base  
 384 cation changes in the plant pool were excluded from the potential inorganic CO<sub>2</sub> removal pool here, as a  
 385 conservative approach we assume that base cations in plants will not reach the ocean. The latter assumption had  
 386 a negligible impact on the potential inorganic CO<sub>2</sub> removal estimate (Table 4).

387 ~~While cations added with the rock feedstock were subtracted to calculate  $W_r$  (Equation 7), they are not subtracted~~  
 388 ~~to calculate the CDR potential as scavenged TA in rock feedstock can also leach to soil water whereby HCO<sub>3</sub><sup>-</sup> is~~  
 389 ~~generated. Last, base cation changes in the plant pool were excluded from the CDR potential pool here, as a~~  
 390 ~~conservative approach we assume that base cations in plants will not reach the ocean. The latter assumption had~~  
 391 ~~a negligible impact on the CDR potential estimate (Table 4).~~

$$392 \quad \text{CDR potential} \left[ \frac{\text{kg CO}_2}{\text{t rock}} \right] = \text{Scavenged TA} \left[ \frac{\text{mol TA}}{\text{g rock}} \right] * \frac{\eta \text{ mol CO}_2}{\text{mol TA}} * \frac{44 \text{g CO}_2}{\text{mol CO}_2} * 1000 \quad (10)$$

$$393 \quad \text{with} \left( \frac{\mu\text{g element}_{i_{\text{pool } j}}}{\text{g dry soil}} \right)_{\text{added with feedstock initially}} = 0$$

393

## 394 2.7 Calculation of the carbonate saturation indices (SIc) using Phreeqc

395 To assess whether carbonate precipitation was theoretically possible during this experiment, we calculated SIc for  
 396 dolomite and calcite. For Mg and Ca the SIc as the logarithm of the ion activity product and the solubility product  
 397 constant if dolomite and calcite (SIc = log IAP/K Minerals have the potential to precipitate when a log SIc >0 is  
 398 reached although substantial oversaturation of calcite (log SIc > 1) without calcite formation is possible in rivers due  
 399 to ion inhibition, e.g. by phosphate (Morse et al., 2007; Zhang et al., 2022). Likewise, they are in equilibrium at a  
 400 log SIc =0 and dissolve if log SIc <0. )-Minerals have the potential to precipitate when a log SIc >0 is reached  
 401 although substantial oversaturation of calcite (log SIc > 1 ) without calcite formation is possible in rivers due to ion  
 402 inhibition, e.g. by phosphate (Morse et al., 2007; Zhang et al., 2022). Likewise, they are in equilibrium at a log SIc  
 403 =0 and dissolve if log SIc <0.The R phreeqc package was used and the phreeqc.dat database was used. As an  
 404 input, the experimental pore water (10 cm depth) composition of Mg and Ca was entered, as well as measured pH

405 and TA. Daily Sic values were calculated by feeding unique combinations of Mg, Ca, pH and into the PHREEQC  
406 solution function for each day.

## 407 408 **2.8 Data analysis**

409 For SIC and elemental stocks in plant biomass, soil pools and soil water export, a linear regression with basalt  
410 application rate as a dependent variable was performed to test for a basalt effect. For measurements that were  
411 repeated in time (pore water and leachate DIC and DOC compositions), a linear mixed model was used with basalt  
412 and time as fixed factors and mesocosm as a random factor using the lme4 R package (version 1.1-33). For  
413 measurements repeated in time, we assessed basalt x time interaction effects and discarded these if not  
414 significant. All analyses were executed in R version 4.3.2. As an additional sensitivity analysis for the determination  
415 of  $W_r$  using the slope of application rates approach described in the main text, we quantified  $W_r$  also for individual  
416 application rates in Fig. S13.

417 [To propagate uncertainty between basalt and controls in Figure 5, averages and standard errors for every replicated](#)  
418 [application rate \(0 or 50 t/ha\) were determined. The average from the 50 t ha<sup>-1</sup> was subtracted with the average](#)  
419 [from the control soil and  \$se = \sqrt{\(se\\_control^2 + se\\_basalt^2\)}\$ . For non-replicated application rates \(10,30, 75,100, 150](#)  
420 [and 200 t/ha,  \$se=0\$ \) the measurement was subtracted from the control soil average and errors were also propagated](#)  
421 [with  \$se = \sqrt{\(se\\_control^2 + se\\_basalt^2\)}\$ .](#)

## 422 **3 Results**

423 Basalt amendment significantly increased DIC and TA in the top soil water (**Figure 4**). TA in soil water correlated  
424 positively with DIC ( $R^2 = 0.68$ ,  $p < 0.01$ , **Fig. S10**). TA was thus generated in the basalt amended soil layer, yet we  
425 did not observe DIC or TA increases with higher basalt application rates in water exported from the soil column [at](#)  
426 [60 cm depth](#) (**Figure 4**). Temporal dynamics show that DIC in top soil pore water gradually increased in time with  
427 higher basalt amendment, while DOC decreased in time with more basalt (**Fig. S7 and Table S4**).

429

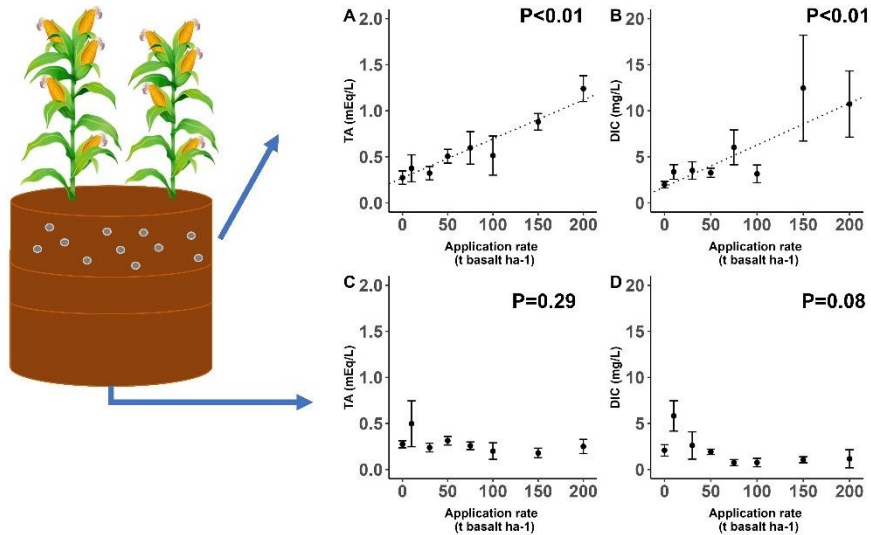


**Figure 4:** [Top soil \(0-20 cm\) pore water \(A\) TA and \(B\) DIC concentrations. Export water \(50 cm depth\) \(C\) TA and \(D\) DIC concentrations. Values represent average concentrations +/- standard error across all sampling occasions over the 101 day duration experiment \(n= 125, 44, 95 and 60 for pore water DIC, TA and leachate DIC and TA concentrations respectively\). Significant trends are indicated with a dotted regression line. Raw data for TA and DIC in function of time is visualized in \[Fig. S7\\(B,D\\)\]\(#\) and \[Fig. S9\\(B,D\\)\]\(#\).](#)

[Top soil \(0-20 cm\) pore water \(A\) TA and \(B\) DIC. Export water \(50 cm depth\) \(C\) TA and \(D\) DIC. Values represent average concentrations +/- SE across all sampling occasions over the 100 day experiment. Significant trends are indicated with a dotted regression line.](#)

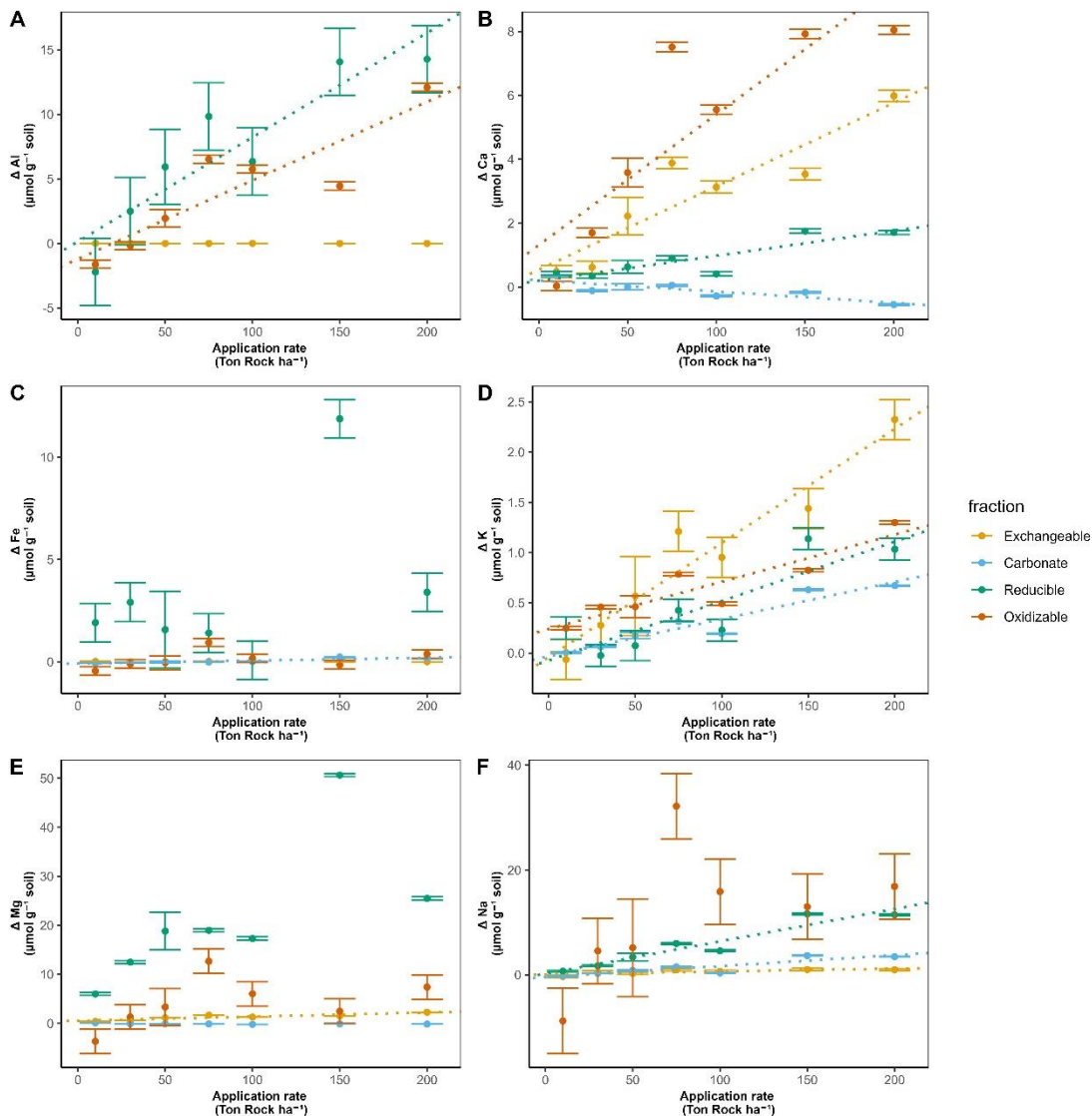
Overall, base cations were mostly retained in the top soil, where Ca significantly increased in the exchangeable, reducible and oxidizable pools with higher basalt addition. Only in the carbonate soil pool, Ca (and also Mg) significantly decreased with more basalt (**Figure 5 and 6**). [With higher rock amendment, Mg accumulated in the top soil exchangeable pool \(p<0.01\). The Mg accumulation in the reducible pool was higher compared to the exchangeable, but the slope was borderline significant \(p=0.07\) due to higher variability with increasing basalt. With higher rock amendment, Mg accumulated in the top soil exchangeable pool \(p<0.01\). The Mg accumulation in the reducible pool was higher compared to the exchangeable, but the slope was borderline significant for the reducible pool \(p=0.07\) due to higher variability with increasing basalt amendment.](#)

Changes in Na followed similar patterns as Mg, as also significantly more Na exchanged in top soil (p=0.02) and a larger signal of reducible Na was found (p<0.01). In contrast with divalent cations, monovalent cations increased in the carbonate fraction if basalt increased (**Figure 5 and 6**). [With more basalt, Al is being found in association with the oxidizable or reducible fraction. With more basalt, Al formed both reducible and oxidizable compounds in top soils, while Si increased only significantly in the oxidizable pool \(p=0.04\) \(Figure 5 and Fig. S15\).](#) Increases in oxidizable Si, Ca, Al with higher basalt addition suggest the formation of mineral-associated organic matter.

In the soil layer just below the soil-basalt mixture (20-30 cm), the cations did not increase significantly in any of the measured soil pools and oxidizable Na, Fe and Mg ~~even~~ decreased significantly (**Fig. S11, Figure 6**). We did not observe significant changes in any element with higher basalt amendment in the 30-50 cm soil layer (**Fig. S12**).

458

459



460

461

462

463

464

465

466

467

468

469

470

471

472

473

474

475

476

477

478

479

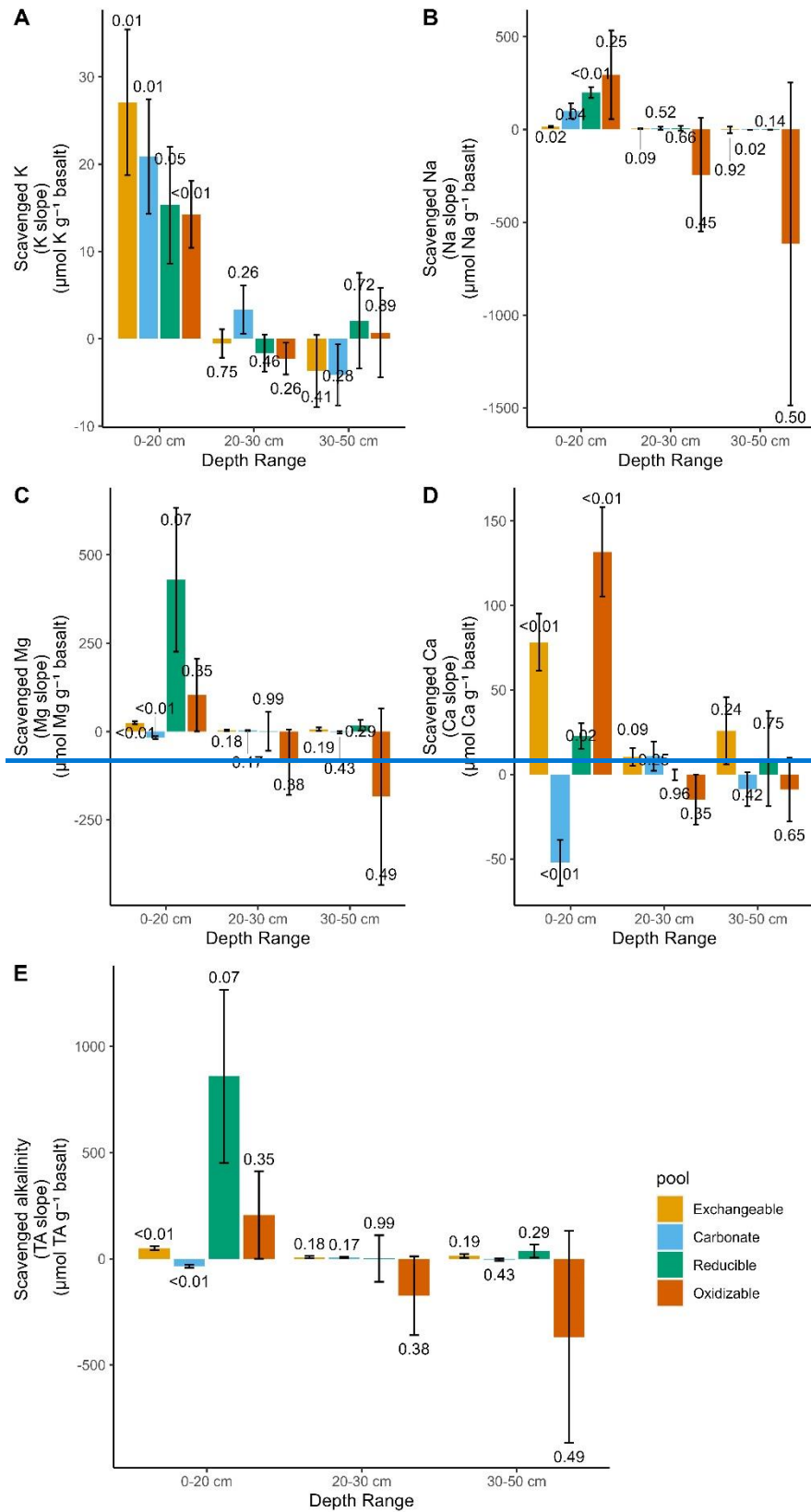
**Figure 5** Change in top soil (0-20 cm) elements relative to the control soil (corrected as in Equation 7), 101 days after basalt amendment, as a function of basalt application rate for (A) Al (B) Ca (C) Fe (D) K (E) Mg and (F) Na for four different soil pools. Dots and error bars represent averages and standard errors. For basalt application rates other than 50 t ha<sup>-1</sup>, error bars correspond to those of the control soils, as these basalt treatments were not replicated and the data are shown as control-normalized results. Significant effects (p<0.05) of basalt application rate on cation concentrations are indicated by dotted linear regression lines. Measurements were repeated on at least four samples per fraction for the control soils (N ≥4 for each fraction) and N=4 for 50 t ha<sup>-1</sup> treatment (fewer than 5 replicates were available due to technical issues). Note that y-axes scales differ among subplots to better visualize small changes for some elements. Unnormalized (raw) data are presented in Fig. S19-21.: Change in top soil (0-20 cm) elements relative to the control soil (corrected as in Equation 7), 101 days after basalt amendment, as a function of basalt application rate for (A) Al (B) Ca (C) Fe (D) K (E) Mg and (F) Na for four different soil pools. Dots and error bars represent averages and SEs. Significant effects (p<0.05) of basalt application rate on cation concentrations are indicated with dotted linear regression lines. Note that y axes absolute values differ for subplots to visualize smaller changes for certain elements. This data was normalized for control soil concentrations, raw data that is not normalized for control soil contribution can be found in Fig. S19-21.

480

From all significant element changes in soil pools, we calculate that 8.4%, 52.1% and 9.4% Of basalt Na, K and Ca were weathered while we do not observe an increase in Mg if we only consider significant (p<0.05) slopes. If we

481 consider all (also  $p > 0.05$ ) regression slopes, the estimates become 48.0%, 10.6%, 9.35% for K, Ca and Mg, while  
 482 Na did not increase in this approach (mass balance per element, see Fig. S234).

483



484  
485

486 **Figure 6:** Equivalent alkalinity uptake 101 days after basalt amendment in different soil pools and depths. P-values  
 487 of linear regressions are shown above and below bar plots of positive and negative changes respectively. Error  
 488 bars represent the standard error that was derived from linear regression. Underlying regressions for slopes of TA  
 489 scavenged by each pool and depth can be found in Fig. S22. Base cation changes in top soil pore water are not  
 490 included in this figure as we only include charge equivalent adsorbed by soil pools here, yet base cations in top soil  
 491 pore water were negligible (see Fig. S24). Equivalent alkalinity uptake 101 days after basalt amendment in different  
 492 soil pools and depths. P-values of linear regressions are shown above and below bar plots of positive and negative  
 493 changes respectively.  
 494 Error bars represent the SE of the mean.  
 495  
 496  
 497  
 498

499 Base cations were not only scavenged by soils, but also by plants. Although two orders of magnitude smaller than  
 500 in soil pools, TA scavenging by plants was higher than soil water exported TA and increased significantly with larger  
 501 basalt amendment ( $p < 0.01$ ) (Figure 7). The increase in base cation charges in plants was attributed to K (81%),  
 502 Ca (11%) and Mg (8%).  
 503

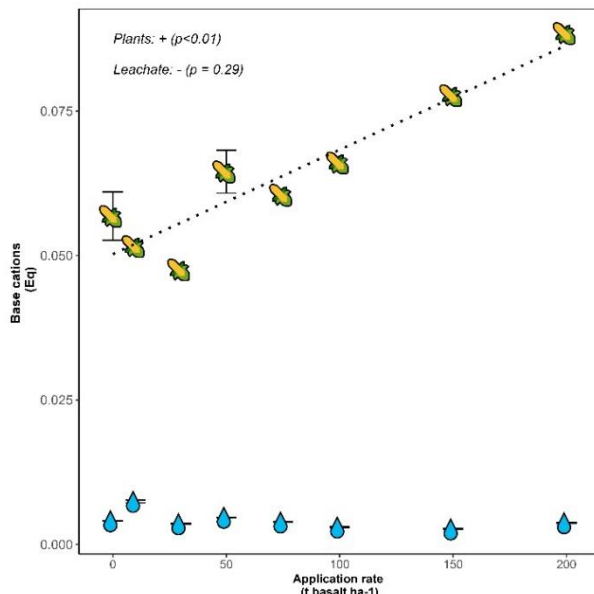


**Figure 7:** Moles of base cation charge equivalent (Eq) per mesocosm after 101 days retained in maize plants (stems, leaves and maize ears), indicated with maize fruit symbols, and flushed with leaching water, indicated with droplets. Error bars represent averages and standard errors ( $n=5$  for both control and  $50 \text{ t ha}^{-1}$  basalt replicates for plant measurements). For leachate TA, a total of 60 measurements were done in total at different dates. Na was not analyzed in plants and is thus not included in the harvested base cations. Errors on leachate TA were small and appear as horizontal lines within the droplets. Raw data for leachate TA measurements can be found in Fig S9D.

526 leachate TA were small and appear as horizontal lines within the droplets. Raw data for leachate TA measurements  
 527 can be found in Fig S9D.

528 **Figure 7:** Moles of base cation charge equivalent (Eq) per mesocosm after 101 days retained in maize plants  
 529 (stems, leaves and corn ears) (indicated with maize fruit symbols) and flushed with leaching water (indicated with  
 530 droplets). Error bars represent averages and SEs. Note that Na was not analyzed in plants and is thus not included  
 531 in the harvested base cations. Errors on leachate TA were small and appear as horizontal lines within the droplets.  
 532  
 533

534 Converting the base cations to moles of equivalent TA and considering only the exchangeable pool as only soil  
 535 cation reservoir we derive a log weathering rate of  $-12.13 \pm 0.34 \text{ mol TA m}^{-2} \text{ rock s}^{-1}$  (Table 4). When we consider  
 536 also the decrease in base cation equivalents in the carbonate pool, the mean estimate decreases to  $-12.23 \text{ mol TA}$   
 537  $\text{m}^{-2} \text{ rock s}^{-1}$ , translating into mean estimated CDR potential/Potential inorganic CO<sub>2</sub> removals of  $0.36\text{-}0.5 \text{ kg CO}_2 \text{ t}$   
 538  $\text{}^1 \text{ basalt}$  (assuming  $\eta=0.5\text{-}0.7$ ). If we include all soil pools and non significant regressions the estimates becomes  
 539 one order of magnitude higher, yet with substantial uncertainty.

540 **Table 4:** Overview of the Wr and CDR potential/potential inorganic CO<sub>2</sub> removal that can be quantified from changes in base  
 541 cations in specific soil pools. Rows where (scavenged) TA increased significantly with increasing basalt amendment are  
 542 indicated in bold.

Soil Pool	Depth	Reservoir	Log Wr (Log mol TA/m <sup>2</sup> basalt /s)	CDR Potential* (kg CO <sub>2</sub> /ton basalt) (η = 0.5)	CDR Potential* (kg CO <sub>2</sub> /ton basalt) (η = 1)
/	/	Plant*	-12.93±0.07	/	/
/	/	Leachate*	Wr<0	/	/
Exchangeable	0-20cm	soil	-12.20±0.41	1.10±0.04	2.21±0.07
Carbonate	0-20cm	soil	Wr<0	-0.75±0.03	-1.50±0.06
Reducible	0-20cm	soil	-10.96±0.21	18.91±1.76	37.82±3.51
Oxidizable	0-20cm	soil	-11.58±0.43	4.53±0.89	9.06±1.77
Exchangeable	20-30cm	soil	-13.02±0.29	0.17±0.02	0.34±0.04
Carbonate	20-30cm	soil	-13.17±0.29	0.12±0.02	0.23±0.03
Reducible	20-30cm	soil	-	-	-
Oxidizable	20-30cm	soil	13.17±50.43	0.02±0.47	0.04±0.95
Exchangeable	30-50cm	soil	Wr<0	-3.82±0.80	-7.56±1.60
Carbonate	30-50cm	soil	-12.76±0.30	0.30±0.04	0.61±0.08
Reducible	30-50cm	soil	Wr<0	-0.10±0.02	-0.21±0.05
Oxidizable	30-50cm	soil	-12.34±1.15	0.79±0.13	1.58±0.27
Exchangeable	0-20	Exchangeable+plant+leachate	-12.13±0.34	1.30±0.04	2.21±0.07
Exchangeable + Carbonate	0-20	Exchangeable+plant+leachate+ carbonate	-12.23±1.05	0.36±0.05	0.71±0.10
All soil pools	All	All soil pools + plant + leachate	-11.11±2.70**	13.17±3.07	26.33±6.13

543 \*For leachates (which represents realized CDR) and also for plants there is no [CDR potential inorganic](#)  
544 [CO<sub>2</sub> removal](#) in this approach.  
545 \*\* Abs (Wr/standard error (Wr)\*LN(10)) was used to propagate the error using the log10 transformation, resulting  
546 in substantial uncertainty for the Wr estimate of all pools.

## 547 4. Discussion

### 548 4.1 Weathering rates and CO<sub>2</sub> removal

549 EW is typically considered as a durable CDR pathway that removes CO<sub>2</sub> from the atmosphere by producing DIC  
550 that is either transported to the ocean (Strefler et al., 2018) or precipitates as carbonates in the soil (Manning et al.,  
551 2013). Here, we observe a clear weathering signal (a TA and DIC increase) in top soil pore water (**Figure 4**). These  
552 TA and DIC increases in the pore water of amended top soil are consistent with recent findings (Holzer et al., 2023;  
553 McDermott et al., 2024; Vienne et al., 2024). [Increased DIC in basalt soils relative to controls may result from  
554 enhanced plant root respiration or DIC exudation or from mineral weathering; our dataset does not allow these  
555 effects to be separated.](#) -DIC did however not leach from our soil columns within this experimental timeframe of 101  
556 days.

557 [Absence of substantial DIC leaching is in line with other short-term recent studies \(Amann et al., 2020; Larkin et al.,  
558 2022; Niron et al., 2024; Vienne et al., 2024\). For example, the log Wr of approximately -13 mol CO<sub>2</sub> m<sup>2</sup> s<sup>-1</sup> quantified  
559 from DIC export after 1 year in a mesocosm trial with 220 ton ha<sup>-1</sup> olivine-rich rock \(Amann et al., 2020\) was about  
560 three orders of magnitude lower than what would be expected from lab-scale weathering studies \(roughly -10,  
561 \(Palandri & Kharaka, 2004\)\).](#)

565  
566 ~~Absence of substantial DIC leaching is in line with other short term recent studies (Amann et al., 2020; Larkin et al.,~~  
567 ~~2022; Niron et al., 2024; Vienne et al., 2024). For example, DIC export after 1 year in a mesocosm trial with 220~~  
568 ~~ton ha<sup>-1</sup> olivine-rich rock was about three orders of magnitude lower than what would be expected from lab-scale~~  
569 ~~weathering shake flask studies (Amann et al., 2020).~~ Vienne et al. (2024), amended soils with 100 ton basalt ha<sup>-1</sup>  
570 and quantified ~~that a~~ CDR from exported TA that was in the same order of magnitude as in the work of Amann et  
571 al. (2020). Although the studies of Amann et al. (2020), Vienne et al. (2024) were relatively short ( $\leq 1$  year) and  
572 used a relatively low water infiltration flux, also a longer (3 year duration) catchment-scale study in Malaysian oil  
573 palm plantations with high annual rainfall ( $>2000$  mm year<sup>-1</sup>) detected no significant increase in TA leaching in the  
574 catchments (Larkin et al., 2022). There may thus be a substantial delay for DIC leaching.

575  
576 This DIC leaching delay can have multiple causes (**Figure 1**); A first possibility is pedogenic carbonate formation.  
577 We observe that solid carbonates did not increase in our experiment, in contrast, SIC even decreased in time.  
578 PHREEQC calculations for our experiment suggest that dolomite and calcite were undersaturated, so that  
579 carbonate dissolution was possible (**Fig. S17**). Saturation states are expected to be low in our experiment because  
580 control soil was undersaturated and dissolved base cations ~~were scavenged by~~ accumulated in other soil pools than  
581 the carbonate pool (**Figure 5 and 6**). A decrease in SIC is in contrast with substantial SIC increases found after  
582 wollastonite rock amendment (Haque et al., 2019, 2020). The observed SIC increase in the latter field study may  
583 be partly attributed to residual carbonates from prior liming activities (Haque et al., 2020), potentially biasing the  
584 results. Thus, not all measured SIC may reflect new carbonate formation in the study of Haque et al. (2020). For  
585 short-term basalt studies, using elemental C analysis, also no significant changes in SIC could be detected  
586 previously (Kelland et al., 2020; Vienne et al., 2022, 2024). In contrast, in the study of Larkin et al. (2022), a relatively  
587 small SIC increase was detected in amended soils, using carbonate pool extractions.

588  
589 While TA was not exported or taken up by soil carbonates here and plant base cation losses were minor (Table 4)  
590 it was retained in top soil where the exchangeable and reducible pools reduced solute TA. We expect cations to be  
591 primarily associated with Fe- and Mn-(oxyhydr)oxides in the reducible pool and with organic matter in the oxidizable  
592 pool, as supported by literature (Tessier et al., 1979); However, the extraction chemicals of this sequential extraction  
593 scheme (hydroxylamine and H<sub>2</sub>O<sub>2</sub>) are known to have a limited specificity and may have also partially targeted  
594 other mineral phases (such as clays) (Ryan et al., 2008), which could explain the elevated Si observed in the topsoil  
595 pools (Fig. S15). In addition, the observed increase of aluminum in association with the reducible soil fraction  
596 indicate the formation of secondary minerals. While we cannot pinpoint the exact Mg-phases formed in our soils,  
597 our results do demonstrate substantial base cation retention in the soil and show that there can be more base cation  
598 losses to soils than to the exchangeable pool alone.

599  
600 Our estimate of log  $W_r$ , derived solely from significant increases in TA uptake at higher basalt amendment rates,  
601 was approximately  $-12 \text{ mol TA m}^{-2} \text{ s}^{-1}$ . This estimate reflects changes in the exchangeable and carbonate soil  
602 pools, plant uptake, and leachate composition. Notably, this value aligns with previous studies that estimated log  $W_r$   
603 values between  $-12$  and  $-11$  based on base cation depletion from the exchangeable pool alone (Kelland et al.,  
604 2020; Reershemius, Kelland, Jordan, et al., 2023; te Pas et al., 2023), as summarized in Vienne et al., (2024). Also  
605 in a batch leaching experiment with  $1 \text{ mM CaCl}_2$  (designed to mimic soil solutions) the quantified log  $W_r$  of basalt  
606 was found to be  $-11$  (Van Der Bauwhede et al., 2024).

607  
608  
609 ~~While TA was not exported or taken up by soil carbonates here and plant base cation losses were minor (Table 4)~~  
610 ~~it was retained in top soil where the exchangeable and pools reduced solute TA. Our log  $W_r$  estimate quantified~~  
611 ~~from significant changes in TA uptake with higher basalt amendment only was approximately  $-12 \text{ mol TA m}^{-2} \text{ s}^{-1}$ .~~  
612 ~~with basalt in soils measuring base cation scavenging only in the exchangeable pool (Kelland et al., 2020;~~  
613 ~~Reershemius et al., 2023; Reynaert et al., 2023; te Pas et al., 2023), where log  $W_r$  was between  $-12$  and  $-11$  (see~~  
614 ~~Table summarized by Vienne et al., (2024)).~~ Estimates from Buckingham et al. (2022), based only on leachates,  
615 gave a much lower log  $W_r$  of  $-15$ , partly due to low water infiltration rates. ~~Even  $W_w$~~  with a high infiltration flux (8000  
616 mm/year), Amann et al. (2022) estimated log  $W_r$  between  $-12.5$  and  $-13.5$  from basalt leachates. This highlights the  
617 importance of including scavenged alkalinity to determine  $W_r$  in soils. When we also include non-significant  
618 regression slopes we derive a mean log  $W_r$  estimate with substantial uncertainty ( $-11.11 \pm 2.70$ )  $\text{mol TA m}^{-2} \text{ s}^{-1}$ . From  
619 individual application rates, we ~~even~~ quantify log  $W_r$  ranging between  $-11$  and  $-10$  (**Fig. S13**); These values are  
620 comparable to those observed in soil-free, laboratory-scale basalt dissolution experiments conducted at  
621 circumneutral pH (Brantley et al., 2008; Gislason & Oelkers, 2003). They also approximate the dissolution rates of  
622 key mineralogical components in basalt (such as plagioclases (between  $-12$  and  $-9$  for Na and Ca endmembers  
623 respectively) and augite ( $-11.97$ )) under room temperature and neutral pH conditions (Gudbrandsson et al., 2011;  
624 Hermanska et al., 2022; Palandri & Kharaka, 2004). ~~these values are comparable to basalt in soil-free shake flask~~  
625 ~~experiments at circumneutral pH (Brantley et al., 2008).~~

626  
627 Although this and other experiments show relatively consistent weathering rates from exchangeable base cations  
628 (comparable to those observed in lab-scale studies) we emphasize that, unlike laboratory conditions where base  
629 cations remain far from equilibrium in excess water, soils experience solid-phase cation scavenging, which  
630 promotes DIC degassing (Figure 1). ~~Although this and other experiments quantify a relative consistent weathering~~  
631 ~~rate from exchangeable bases and derived rates are comparable to shake flask experiments, we emphasize that~~  
632 ~~unlike in shake flask experiments where base cations remain irreversibly dissolved, in soils, solid-phase base cation~~  
633 ~~scavenging causes DIC degassing (Figure 1).~~ From the sum of significant TA slopes we calculate a relatively low  
634 ~~CDR potential~~ Potential inorganic  $\text{CO}_2$  removal, equalling to ~~only~~ approximately  $0.36\text{-}0.71$   $0.4\text{-}0.5$   $\text{kg CO}_2 \text{ ton}^{-1}$   
635 basalt or  $0.018\text{-}0.036$   $0.020\text{-}0.025$   $\text{tCO}_2 \text{ ha}^{-1}$  for a basalt application rate of  $50 \text{ t ha}^{-1}$  (Table 4). Also the highest  
636 possible potential inorganic  $\text{CO}_2$  removal realized within this experimental timeframe is modest; Including also non-  
637 significant TA increases and assuming  $\eta = 1$ , the potential inorganic  $\text{CO}_2$  removal is quantified to be  $26.33 \pm 6.13 \text{ kg}$

638 [CO<sub>2</sub> ton<sup>-1</sup> basalt \(Table 4\)](#). We emphasize that a ~~CDR potential~~[Potential inorganic CO<sub>2</sub> removal](#) is a maximum  
639 ~~inorganic CDR~~[inorganic CO<sub>2</sub> removal](#) that can be realized with the delivered amount of base cation weathering as  
640 strong acids associated with fertilizers (such as nitric acid and sulphuric acid), or organic acids and not carbonic  
641 acid may have initially weathered silicate rock which does not lead to a CDR [within the soil system](#) (McDermott et  
642 al., 2024; Taylor et al., 2021). [Moreover, life-cycle emissions for mining, grinding and transporting rock are typically](#)  
643 [in the same order of magnitude as our relatively low Potential inorganic CO<sub>2</sub> removal \(Lefebvre et al., 2019\)](#).

644

645

646 ~~Furthermore,~~ for climate change mitigation, not only the amount of ~~CDR potential~~[Potential inorganic CO<sub>2</sub> removal](#)  
647 is important, but also the timescale at which this CDR is realized (Kanzaki et al., 20254). [A mass balance of base](#)  
648 [cations indicates that exported TA was negligible compared to base cation charges that were retained in the soil](#)  
649 [over the timeframe of our experiment \(101 days\) \(Table 4\)](#).

650 ~~A mass balance of TA shows that exported TA was negligible compared to scavenged TA that was retained in the~~  
651 ~~soil (Table 4)~~. As long as TA is retained in soil pools, ~~inorganic CDR~~[inorganic CO<sub>2</sub> removal](#) through DIC export is  
652 delayed as equivalent amounts of protons have then been released into the soil water to maintain charge balance  
653 (**Figure 1**). Realization of this delayed ~~inorganic CDR~~[inorganic CO<sub>2</sub> removal](#) depends on liberation of base cations  
654 from these soil pools and their transport out of the soil, charge-balanced by HCO<sub>3</sub><sup>-</sup>. This export may take decades  
655 or longer, depending on the circumstances (Kanzaki et al., 2024).

656

657 The realization of CDR may be ~~even~~ further delayed through the formation of base cation bearing clay minerals.  
658 Clay formation has previously been suggested for EW application based on changes in soil water Ge/Si ratios and  
659 Si isotopes (Vienne et al., 2024) [and also based on Li isotope measurements \(Pogge von Strandmann et al., 2022\)](#).  
660 These measurements indicated basalt induced clay formation, but it remains unclear what type of clays were formed  
661 and hence what the effect on ~~inorganic CDR~~[inorganic CO<sub>2</sub> removal](#) may be. In the best case for the ~~inorganic~~  
662 ~~CDR~~[inorganic CO<sub>2</sub> removal](#) lag, the formed clays are 1:1 phyllosilicates [such as kaolinite that do not sequester](#)  
663 [base cations](#). In this case, DIC leaching is only retarded by base cation exchange. Worst case for the ~~inorganic~~  
664 ~~CDR~~[inorganic CO<sub>2</sub> removal](#) time lag, the formed secondary minerals bear substantial amounts of base cations  
665 such as chlorite or chrysotile. These clays exhibit a log W<sub>r</sub> between -12 and -12.5 at neutral pH (Palandri & Kharaka,  
666 2004b), so that dissolution within decadal timescales is unlikely (Bullock et al., 2022).

667

668 ~~To investigate whether base cation bearing clays could be forming in the top soil reducible pool in this experiment,~~  
669 ~~we compared Mg/Si and Al/Si ratios with common clays (Fig. S22). We could not find a good stoichiometric match~~  
670 ~~between reducible pool and known crystalline clay phases. Still, amorphous clay precursors with deviating~~  
671 ~~stoichiometry could be present in the reducible pool and crystalline clays could also be hiding in the unassessed~~  
672 ~~residual soil pool that remains after the sequential extraction procedure (Niron et al., 2024). Ryan et al., (2008)~~  
673 ~~showed that <20% of crystalline clay minerals can be extracted with the similar BCR extraction scheme and an~~  
674 ~~additional aqua regia digest is required to measure clays. We therefore suggest for future research to add an~~  
675 ~~additional clay targeting leach.~~

676

677 Although unfavourable for ~~inorganic CDR~~[inorganic CO2 removal](#), if base cation bearing secondary clay minerals  
678 would form, they can increase SOC (Georgiou et al., 2022; Heckman et al., 2022; Steinwider et al., 2025).  
679 Georgiou et al. (2022) ~~refer to base-cation bearing clays (e.g. smectitic or illitic clays) refers to the latter clays~~ as  
680 'high-activity minerals' due to their higher SOM stabilization capacity compared to secondary minerals that do not  
681 contain base cations (i.e., 'low-activity minerals', with a lower CEC such as kaolinite). Both high- and low-activity  
682 minerals can adsorb DOC and form mineral-associated organic matter-C (MAOM-C), which is believed to have a  
683 relatively high permanence (decades-centuries) in soils (Lal et al., 2020). Besides mineral surface however,  
684 plant inputs can also limit SOC accrual. In the latter case, SOC stocks can only increase if belowground plant C  
685 inputs increase, which could follow from increases in exchangeable bases or pH (Haque et al., 2019; Shamshuddin  
686 et al., 2011). Nonetheless, increases in decomposition can also stimulate SOC losses if rock dust increases soil pH  
687 (Klemme et al., 2022). ~~The response of SOC to EW is thus prone to several contrasting mechanisms and requires~~  
688 ~~further investigation.~~

689

690

691

692

693

694

695

696

697

#### 4.2 Implications for monitoring ~~inorganic CDR~~[inorganic CO2 removal](#)

698 Different base cation monitoring strategies are possible. A first option is to quantify TA in soil water ([Clarkson et](#)  
699 ~~al., 2024~~) (~~Isometric, 2024~~). A disadvantage is however that soil water samples have to be sampled across the soil  
700 depth. Alternatively, TA could be only monitored in top soil, yet then uncertain TA leaching models must be used  
701 (Kanzaki et al., 2024). ~~To calibrate TA leaching models, soil measurements in depth profiles could be used. To~~  
702 ~~decrease the uncertainty of TA leaching models, soil measurements in depth profiles could be used to calibrate~~  
703 ~~these models.~~

704

705 [A first soil measurement approach is a total cation accounting approach, which quantifies the loss of base cations](#)  
706 [from top soils. However, this approach only focuses on the top soil and fails to account for physical cation transport](#)  
707 [from top soils due to erosion or vertical feedstock transport via infiltration or bioturbation. Alternatively, in a](#)  
708 [mobile/immobile tracer element approach \(often named 'TiCat' by the EW community\), cation losses from amended](#)  
709 [top soils are quantified along with immobile tracers, which can account for cation losses through bioturbation or](#)  
710 [erosion](#) (Reershemius, ~~Kolland, Davis~~, et al., 2023). [Nonetheless the disadvantage of TiCat is that it does not track](#)  
711 [potential TA scavenging \(e.g. by organic matter or clays\) at larger depth. Our Potential inorganic CO2 removal](#)  
712 [estimate will thus differ from a Potential inorganic CO2 removal estimates quantified using a TiCat approach.](#)

713  
714  
715  
716  
717  
718  
719  
720  
721  
722  
723  
724  
725  
726  
727  
728  
729  
730  
731  
732  
733  
734  
735  
736  
737  
738  
739  
740  
741  
742  
743  
744  
745  
746  
747

~~A first soil measurement approach is a mobile/immobile element approach, which tracks cation losses from amended top soils (Reershemius et al., 2023). However, this approach only focuses on the top soil and fails to account for cation loss from top soils due to erosion or vertical feedstock transport via infiltration or bioturbation (Reershemius et al., 2023). In addition this approach does not track potential TA scavenging by organic matter or clay formation at larger depth.~~

Alternatively, entire depth profiles could be analyzed to spatially calibrate TA leaching models. The Isometric protocol already includes the analysis of the exchangeable soil pool as a requirement (Isometric, 2024). Adding also the carbonate, reducible and oxidizable soil pools to the analysis could make base cation mass balancing more complete. These protocols could calibrate predictive TA leaching models spatially. In addition there is an opportunity to quantify soil organic carbon (SOC) and MAOM-C changes in the same samples, which have recently gained traction in EW research due to their role in stabilizing SOM (Buss et al., 2024; Sokol et al., 2024; Xu et al., 2024). Integration of these measurements can provide more accurate estimates of the climate impact of EW, but should take into account the difference in permanence of inorganic and organic carbon stocks.

However, this [MRV monitoring](#) approach involves complexities such as feedstock correction, leaching solution strength and soil heterogeneity. Although correcting for pre-weathered elements was crucial in this study, it assumes perfect mixing based on a silicate-to-soil ratio. This correction was particularly significant for carbonate and reducible soil pools, where for some base cations, over half of the cation increase with basalt amendment originated from feedstock addition and not from weathering (**Fig. S18**). An alternative approach could involve creating time series from sequential extraction data and quantifying base cation changes [based on the change in time between multiple measurements taken after rock amendment.](#) ~~based on the slope between two measurements taken after rock amendment.~~

~~As discussed in the previous section, another key challenge is that the fate of base cations may remain uncertain if strongly bound crystalline organo-minerals (see Lopez-Sangil & Rovira, 2013) form that are unextractable by the Tessier scheme. Such processes may have contributed to the observed decrease in oxidizable elements at larger depth, although this could also be an artefact of the applied extraction procedure.. As discussed in the previous section, another key challenge is that the fate of base cations may remain uncertain if strongly bound crystalline secondary minerals form that are unextractable by the Tessier scheme.~~ Pogge von Strandmann et al. (2022) proposed substituting the H<sub>2</sub>O<sub>2</sub> leaching step of the Tessier scheme with a dilute HCl leach, which is thought to extract clays as well. Alternatively, post-extraction analysis of residual solids using techniques such as XRD or QEMSCAN may be necessary to rigorously assess changes in rock mineralogy (Mason et al., 2022). Although deep soil core sampling and extensive mineralogical analysis are resource-intensive and not feasible for large-scale

748 application, this monitoring strategy could be valuable during the initial adoption of EW in targeted 'measure-all'  
749 experiments, as reliable TA leaching models require extensive calibration.

750

## 751 5. Conclusions

752 This study presents a detailed examination of EW and its effectiveness as a climate mitigation technique, revealing  
753 both its potentials and limitations. A novel aspect of this work is the in-depth investigation of entire soil profiles for  
754 base cations in different soil fractions, paired with soil water TA monitoring. We highlight the value of sequential  
755 extractions as a method for monitoring base cations throughout soil profiles for calibrating TA leaching models.

756 ~~Our findings indicate that basalt-based enhanced weathering may not immediately lead to the inorganic CO<sub>2</sub>~~  
757 ~~removal previously anticipated in projections and IPCC reports (Babiker et al., 2022; Minx et al., 2018). Our results~~  
758 ~~suggest that EW using basalt amendments may not yield the immediate inorganic carbon dioxide removal (CDR)~~  
759 ~~benefits previously anticipated.~~ We observed rock weathering without ~~inorganic CDR~~inorganic CO<sub>2</sub> removal ;  
760 despite the absence of DIC leaching or carbonate precipitation, exchangeable bases increased with higher basalt  
761 amendments, ~~proving~~demonstrating that rock weathering occurred. Additionally, we observed a borderline  
762 significant but substantial increase in base cations in the reducible topsoil pool with greater basalt application, which  
763 may further suppress TA leaching.~~Additionally, we observed a borderline significant yet substantial increase in~~  
764 ~~reducible bases in top soils with more basalt, which may further retard TA leaching.~~

765 As base cation exchange increased with higher basalt amendments, we infer that greater application rates may  
766 further delay the release of DIC from soil minerals to surface waters. However, in practice, EW is typically applied  
767 at application rates below 30 t ha<sup>-1</sup>. These lower, more practical rates may also enhance inorganic CO<sub>2</sub> removal  
768 effectiveness by reducing lag times for DIC release.~~As base cation exchange increased with higher basalt~~  
769 ~~amendments, we infer that the eventual release of DIC from soil minerals into surface waters will be further delayed~~  
770 ~~with higher rock applications. This renders high basalt application rates less effective as a strategy for achieving~~  
771 ~~rapid inorganic CDR~~inorganic CO<sub>2</sub> removal .—It remains unclear if clays were formed here and whether EW can  
772 deliver CDR within the urgent decadal timeframe needed to mitigate climate change. Despite its limitations for short-  
773 term ~~inorganic CDR~~inorganic CO<sub>2</sub> removal, the generated secondary minerals and increased cation exchange  
774 capacity (CEC) could enhance plant productivity and soil organic carbon (SOC) retention in soils, contributing to  
775 long-term soil health, fertility, and potentially carbon sequestration beyond inorganic pathways.

## 776 Acknowledgements

777 We thank Anne Cools, Steven Joosen and Anke De Boeck for their assistance with ICP-OES for sequential  
778 extraction samples and Anthony De Schutter to characterize basalt using XRD. We thank DURUBAS to provide  
779 basalt and provide the XRF material data sheet. We thank Tom Cox for fruitful discussions. We acknowledge the

780 use of Microsoft Copilot to improve the English of this manuscript. This research was supported by the Research  
781 Foundation— Flanders (FWO) [1S06325N], 1174925N] and [G000821N] (Biotic controls of the potential of  
782 enhanced silicate weathering for land-based climate change mitigation). We also acknowledge support of the  
783 UPSURGE project, which has received funding from the European Union's Horizon 2020 research and innovation  
784 program under grant agreement No 101003818.

785

786

## 787 Author contribution

788 AV: research conceptualization, data gathering, development methodology, data analysis and writing. PF: conceptualized  
789 sequential extraction methodology, writing and discussion. JR: research conceptualization, data gathering. TJS: writing and  
790 discussion. TR: writing and discussion. RP: data gathering, rock characterization and writing. JH: writing and discussion. HN:  
791 development extraction methodology, writing and discussion. MPE: elemental C measurements and proofreading. LS: writing,  
792 development methodology and discussion. LB: writing and discussion. SV: supervising research, conceptualization, writing and  
793 discussion.

## 794 Data and code availability

795 Data and code used in this manuscript are freely available at: <https://zenodo.org/records/15129984>

796

## 797 References

- 798 Amann, T., & Hartmann, J. (2022). Carbon Accounting for Enhanced Weathering. *Frontiers in Climate*, 4(May), 1–  
799 9. <https://doi.org/10.3389/fclim.2022.849948>
- 800 Amann, T., Hartmann, J., Hellmann, R., Pedrosa, E. T., & Malik, A. (2022). Enhanced weathering potentials—the  
801 role of in situ CO<sub>2</sub> and grain size distribution. *Frontiers in Climate*, 4.  
802 <https://doi.org/10.3389/fclim.2022.929268>
- 803 Amann, T., Hartmann, J., Struyf, E., De Oliveira Garcia, W., Fischer, E. K., Janssens, I., Meire, P., & Schoelynck,  
804 J. (2020). Enhanced Weathering and related element fluxes - A cropland mesocosm approach.  
805 *Biogeosciences*, 17(1), 103–119. <https://doi.org/10.5194/bg-17-103-2020>
- 806 Barker, S. (2013). Dissolution of Deep-Sea Carbonates. In *Encyclopedia of Quaternary Science* (2nd ed., Vol. 2,  
807 Issue 2002). Elsevier B.V. <https://doi.org/10.1016/B978-0-444-53643-3.00289-2>
- 808 Brantley, S. L., White, A. F., & Kubicki, J. D. (2008). Kinetics of water-rock interaction. In *Kinetics of Water-Rock*  
809 *Interaction* (Issue January). <https://doi.org/10.1007/978-0-387-73563-4>
- 810 Buckingham, F. L., Henderson, G. M., Holdship, P., & Renforth, P. (2022). Applied Geochemistry Soil core study  
811 indicates limited CO<sub>2</sub> removal by enhanced weathering in dry croplands in the UK. *Applied Geochemistry*,  
812 147(October), 105482. <https://doi.org/10.1016/j.apgeochem.2022.105482>
- 813 Bullock, L. A., Yang, A., & Darton, R. C. (2022). Kinetics-informed global assessment of mine tailings for CO<sub>2</sub>  
814 removal. *Science of The Total Environment*, 808, 152111. <https://doi.org/10.1016/j.scitotenv.2021.152111>
- 815 Buss, W., Hasemer, H., Ferguson, S., & Borevitz, J. (2024). Stabilisation of soil organic matter with rock dust  
816 partially counteracted by plants. *Global Change Biology*, 30(1), 1–14. <https://doi.org/10.1111/gcb.17052>
- 817 Clarkson, M. O., Larkin, C. S., Swoboda, P., Reershemius, T., Suhrhoff, T. J., Maesano, C. N., & Campbell, J. S.  
818 (2024). A review of measurement for quantification of carbon dioxide removal by enhanced weathering in soil.  
819 *Frontiers in Climate*, 6(June). <https://doi.org/10.3389/fclim.2024.1345224>
- 820 Dietzen, C., Harrison, R., & Michelsen-Correa, S. (2018). Effectiveness of enhanced mineral weathering as a carbon  
821 sequestration tool and alternative to agricultural lime: An incubation experiment. *International Journal of*  
822 *Greenhouse Gas Control*, 74(January), 251–258. <https://doi.org/10.1016/j.ijggc.2018.05.007>
- 823 Fuss, S., Lamb, W. F., Callaghan, M. W., Hilaire, J., Creutzig, F., Amann, T., Beringer, T., De Oliveira Garcia, W.,  
824 Hartmann, J., Khanna, T., Luderer, G., Nemet, G. F., Rogelj, J., Smith, P., Vicente, J. V., Wilcox, J., Del Mar  
825 Zamora Dominguez, M., & Minx, J. C. (2018). Negative emissions - Part 2: Costs, potentials and side effects.  
826 *Environmental Research Letters*, 13(6). <https://doi.org/10.1088/1748-9326/aabf9f>
- 827 Gao, Y., Lu, Y., Wu, M., Liang, E., Li, Y., Zhang, D., Yin, Z., Ren, X., Dai, Y., Deng, D., & Chen, J. (2016). Ability to  
828 remove Na<sup>+</sup> and retain K<sup>+</sup> correlates with salt tolerance in two maize inbred lines seedlings. *Frontiers in Plant*  
829 *Science*, 7(NOVEMBER2016), 1–15. <https://doi.org/10.3389/fpls.2016.01716>

- 830 Georgiou, K., Jackson, R. B., Vindušková, O., Abramoff, R. Z., Ahlström, A., Feng, W., Harden, J. W., Pellegrini, A.  
831 F. A., Polley, H. W., Soong, J. L., Riley, W. J., & Torn, M. S. (2022). Global stocks and capacity of mineral-  
832 associated soil organic carbon. *Nature Communications*, 13(1), 1–12. <https://doi.org/10.1038/s41467-022-31540-9>  
833
- 834 Gislason, S. R., & Oelkers, E. H. (2003). Mechanism, rates, and consequences of basaltic glass dissolution: II. An  
835 experimental study of the dissolution rates of basaltic glass as a function of pH and temperature. *Geochimica  
836 et Cosmochimica Acta*, 67(20), 3817–3832. [https://doi.org/10.1016/S0016-7037\(00\)00176-5](https://doi.org/10.1016/S0016-7037(00)00176-5)
- 837 Gudbrandsson, S., Wolff-Boenisch, D., Gislason, S. R., & Oelkers, E. H. (2011). An experimental study of crystalline  
838 basalt dissolution from 2pH11 and temperatures from 5 to 75°C. *Geochimica et Cosmochimica Acta*, 75(19),  
839 5496–5509. <https://doi.org/10.1016/j.gca.2011.06.035>
- 840 Haque, F., Santos, R. M., & Chiang, Y. W. (2020). Optimizing Inorganic Carbon Sequestration and Crop Yield With  
841 Wollastonite Soil Amendment in a Microplot Study. *Frontiers in Plant Science*, 11(July), 1–12.  
842 <https://doi.org/10.3389/fpls.2020.01012>
- 843 Haque, F., Santos, R. M., Dutta, A., Thimmanagari, M., & Chiang, Y. W. (2019). Co-Benefits of Wollastonite  
844 Weathering in Agriculture: CO<sub>2</sub> Sequestration and Promoted Plant Growth [Research-article]. *ACS Omega*,  
845 4(1), 1425–1433. <https://doi.org/10.1021/acsomega.8b02477>
- 846 Heckman, K., Hicks Pries, C. E., Lawrence, C. R., Rasmussen, C., Crow, S. E., Hoyt, A. M., von Fromm, S. F., Shi,  
847 Z., Stoner, S., McGrath, C., Beem-Miller, J., Berhe, A. A., Blankinship, J. C., Keiluweit, M., Marin-Spiotta, E.,  
848 Monroe, J. G., Plante, A. F., Schimel, J., Sierra, C. A., ... Wagai, R. (2022). Beyond bulk: Density fractions  
849 explain heterogeneity in global soil carbon abundance and persistence. *Global Change Biology*, 28(3), 1178–  
850 1196. <https://doi.org/10.1111/gcb.16023>
- 851 Holzer, I. O., Nocco, M. A., & Houlton, B. Z. (2023). Direct evidence for atmospheric carbon dioxide removal via  
852 enhanced weathering in cropland soil. *Environmental Research Communications*, 5(10).  
853 <https://doi.org/10.1088/2515-7620/acfd89>
- 854 Isometric. (2024). *Isometric ERW standard*.
- 855 Janssens, I. A., Roobroeck, D., Sardans, J., Obersteiner, M., Peñuelas, J., Richter, A., Smith, P., Verbruggen, E.,  
856 & Vicca, S. (2022). *Negative erosion and negative emissions : Combining multiple land-based carbon dioxide  
857 removal techniques to rebuild fertile topsoils and enhance food production*.
- 858 Kalinichev, A. G., Iskrenova-Tchoukova, E., Ahn, W. Y., Clark, M. M., & Kirkpatrick, R. J. (2011). Effects of Ca<sup>2+</sup>  
859 on supramolecular aggregation of natural organic matter in aqueous solutions: A comparison of molecular  
860 modeling approaches. *Geoderma*, 169, 27–32. <https://doi.org/10.1016/j.geoderma.2010.09.002>
- 861 Kanzaki, Y., Planavsky, N., Zhang, S., Jordan, J., & Christopher, T. (2024a). Soil cation storage as a key control on  
862 the timescales of carbon dioxide removal through enhanced weathering. *ESS Open Archive*, 1–19.
- 863 Kanzaki, Y., Planavsky, N., Zhang, S., Jordan, J., & Christopher, T. (2024b). *Soil cation storage as a key control on  
864 the timescales of carbon dioxide removal through enhanced weathering*.
- 865 Katarzyna A. Kowalczyk, Thorben Amann, Jessica Strefler, M.-E., Vorrath, Jens Hartmann, Serena De Marco, Phil  
866 Renforth, S., & Foteinis, E. K. (2024). Marine Carbon Dioxide Removal by alkalization should no longer be  
867 overlooked. *Environmental Research Letters*, December 2016, 11–14.
- 868 Kelland, M. E., Wade, P. W., Lewis, A. L., Taylor, L. L., Sarkar, B., Andrews, M. G., Lomas, M. R., Cotton, T. E. A.,  
869 Kemp, S. J., James, R. H., Pearce, C. R., Hartley, S. E., Hodson, M. E., Leake, J. R., Banwart, S. A., &  
870 Beerling, D. J. (2020). Increased yield and CO<sub>2</sub> sequestration potential with the C<sub>4</sub> cereal Sorghum bicolor  
871 cultivated in basaltic rock dust-amended agricultural soil. *Global Change Biology*, 26(6), 3658–3676.  
872 <https://doi.org/10.1111/gcb.15089>
- 873 Klemme, A., Rixen, T., Müller, M., Notholt, J., & Warneke, T. (2022). Destabilization of carbon in tropical peatlands  
874 by enhanced weathering. *Communications Earth and Environment*, 3(1), 1–9.  
875 <https://doi.org/10.1038/s43247-022-00544-0>
- 876 Larkin, C. S., Andrews, M. G., Pearce, C. R., Yeong, K. L., Beerling, D. J., Bellamy, J., Benedick, S., Freckleton, R.  
877 P., Goring-harford, H., Sadekar, S., & James, R. H. (2022). *Quantification of CO removal in a large-scale  
878 enhanced weathering field trial on an oil palm plantation in Sabah , Malaysia*.
- 879 Lavallee, J. M., Soong, J. L., & Cotrufo, M. F. (2020). Conceptualizing soil organic matter into particulate and  
880 mineral-associated forms to address global change in the 21st century. *Global Change Biology*, 26(1), 261–  
881 273. <https://doi.org/10.1111/gcb.14859>
- 882 Lefebvre, D., Goglio, P., Williams, A., Manning, D. A. C., Carlos, A., Azevedo, D., Bergmann, M., Meersmans, J.,  
883 & Smith, P. (2019). Assessing the potential of soil carbonation and enhanced weathering through Life Cycle

- 884 Assessment: A case study for Sao Paulo State, Brazil. *Journal of Cleaner Production*, 233, 468–481.  
885 <https://doi.org/10.1016/j.jclepro.2019.06.099>
- 886 Lopez-Sangil, L., & Rovira, P. (2013). Sequential chemical extractions of the mineral-associated soil organic matter:  
887 An integrated approach for the fractionation of organo-mineral complexes. *Soil Biology and Biochemistry*, 62,  
888 57–67. <https://doi.org/10.1016/j.soilbio.2013.03.004>
- 889 Manning, D. A. C., Renforth, P., Lopez-Capel, E., Robertson, S., & Ghazireh, N. (2013). Carbonate precipitation in  
890 artificial soils produced from basaltic quarry fines and composts: An opportunity for passive carbon  
891 sequestration. *International Journal of Greenhouse Gas Control*, 17, 309–317.  
892 <https://doi.org/10.1016/j.ijggc.2013.05.012>
- 893 Mason, J., Lin, E., Grono, E., & Denham, T. (2022). QEMSCAN® analysis of clay-rich stratigraphy associated with  
894 early agricultural contexts at Kuk Swamp, Papua New Guinea. *Journal of Archaeological Science: Reports*,  
895 42(February), 103356. <https://doi.org/10.1016/j.jasrep.2022.103356>
- 896 Matylda Hermanska, Martin J. Voigt, Chiara Marieni, Julien Declercq, E. O. (2022). *A comprehensive and internally  
897 consistent mineral dissolution rate database: Part I: Primary silicate minerals and glasses*. 597(July 2021).  
898 <https://doi.org/10.1016/j.chemgeo.2022.120807>
- 899 McDermott, F., Bryson, M., Magee, R., & van Acken, D. (2024). Enhanced weathering for CO<sub>2</sub> removal using  
900 carbonate-rich crushed returned concrete; a pilot study from SE Ireland. *Applied Geochemistry*, 169(June),  
901 106056. <https://doi.org/10.1016/j.apgeochem.2024.106056>
- 902 Minx, J. C., Lamb, W. F., Callaghan, M. W., Fuss, S., Hilaire, J., Creutzig, F., Amann, T., Beringer, T., De Oliveira  
903 Garcia, W., Hartmann, J., Khanna, T., Lenzi, D., Luderer, G., Nemet, G. F., Rogelj, J., Smith, P., Vicente  
904 Vicente, J. L., Wilcox, J., & Del Mar Zamora Dominguez, M. (2018). Negative emissions - Part 1: Research  
905 landscape and synthesis. *Environmental Research Letters*, 13(6). <https://doi.org/10.1088/1748-9326/aabf9b>
- 906 Morse, J. W., Arvidson, R. S., & Lüttge, A. (2007). Calcium carbonate formation and dissolution. *Chemical Reviews*,  
907 107(2), 342–381. <https://doi.org/10.1021/cr050358j>
- 908 Navarre-Sitchler, A., & Brantley, S. (2007). Basalt weathering across scales. *Earth and Planetary Science Letters*,  
909 261(1–2), 321–334. <https://doi.org/10.1016/j.epsl.2007.07.010>
- 910 Niron, H., Vienne, A., Frings, P., Poetra, R., & Vicca, S. (2024). Exploring the synergy of enhanced weathering and  
911 *Bacillus subtilis*: A promising strategy for sustainable agriculture. *Global Change Biology*, 30(9), 1–18.  
912 <https://doi.org/10.1111/gcb.17511>
- 913 Noah Sokol, Jaeun Sohng, Kimber Moreland, Eric Slessarev, Heath Goertzen, Radomir Schmidt, Sandipan  
914 Samaddar, Iris Holzer, Maya Almaraz, Emily Geoghegan, Benjamin Houlton, Isabel Montañez, Jennifer Pett-  
915 Ridge, K. S. (2024). *Reduced accrual of mineral-associated organic matter after two years of enhanced rock  
916 weathering in cropland soils, though no net losses of soil organic carbon*. 1–37.
- 917 Öquist, M. G., Wallin, M., Seibert, J., Bishop, K., & Laudon, H. (2009). Dissolved Inorganic Carbon Export Across  
918 the Soil / Stream Interface and Its Fate in a Boreal Headwater Stream. *Environmental Science & Technology*,  
919 43(19), 7364–7369.
- 920 Palandri, J. L., & Kharaka, Y. K. (2004a). A compilation of rate parameters of water-mineral interaction kinetics for  
921 application to geochemical modeling. *USGS Open File Report, 2004–1068*, 71. [http://www.dtic.mil/cgi-  
922 bin/GetTRDoc?Location=U2&doc=GetTRDoc.pdf&AD=ADA440035](http://www.dtic.mil/cgi-bin/GetTRDoc?Location=U2&doc=GetTRDoc.pdf&AD=ADA440035)
- 923 Palandri, J. L., & Kharaka, Y. K. (2004b). A compilation of rate parameters of water-mineral interaction kinetics for  
924 application to geochemical modeling. *USGS Open File Report, 2004–1068*(December 2013), 71.  
925 [http://www.dtic.mil/cgi-  
bin/GetTRDoc?Location=U2&doc=GetTRDoc.pdf&AD=ADA440035](http://www.dtic.mil/cgi-bin/GetTRDoc?Location=U2&doc=GetTRDoc.pdf&AD=ADA440035)
- 926 Poeplau, C., Don, A., Six, J., Kaiser, M., Benbi, D., Chenu, C., Cotrufo, M. F., Derrien, D., Gioacchini, P., Grand,  
927 S., Gregorich, E., Griepentrog, M., Gunina, A., Haddix, M., Kuzyakov, Y., Kühnel, A., Macdonald, L. M.,  
928 Soong, J., Trigalet, S., ... Nieder, R. (2018). Isolating organic carbon fractions with varying turnover rates in  
929 temperate agricultural soils – A comprehensive method comparison. *Soil Biology and Biochemistry*,  
930 125(April), 10–26. <https://doi.org/10.1016/j.soilbio.2018.06.025>
- 931 Pogge von Strandmann, P. A. E., Liu, X., Liu, C. Y., Wilson, D. J., Hammond, S. J., Tarbuck, G., Aristilde, L.,  
932 Krause, A. J., & Fraser, W. T. (2022). Lithium isotope behaviour during basalt weathering experiments  
933 amended with organic acids. *Geochimica et Cosmochimica Acta*, 328, 37–57.  
934 <https://doi.org/10.1016/j.gca.2022.04.032>
- 935 Power, I. M., Hatten, V. N. J., Guo, M., Rausis, K., & Klyn-hesselink, H. (2025). Are enhanced rock weathering rates  
936 overestimated? A few geochemical and mineralogical pitfalls. *Frontiers in Climate*, 6(January), 1–9.  
937 <https://doi.org/10.3389/fclim.2024.1510747>

- 938 Reershemius, T., Kelland, M. E., Davis, I. R., D'Ascanio, R., Kalderon-Asael, B., Asael, D., Epihov, D. E., Beerling,  
939 D. J., Reinhard, C. T., & Planavsky, N. J. (2023). *A new soil-based approach for empirical monitoring of*  
940 *enhanced rock weathering rates*. <http://arxiv.org/abs/2302.05004>
- 941 Reershemius, T., Kelland, M. E., Jordan, J. S., Davis, I. R., D'Ascanio, R., Kalderon-Asael, B., Asael, D., Suhrhoff,  
942 T. J., Epihov, D. Z., Beerling, D. J., Reinhard, C. T., & Planavsky, N. J. (2023). Initial Validation of a Soil-  
943 Based Mass-Balance Approach for Empirical Monitoring of Enhanced Rock Weathering Rates. *Environmental*  
944 *Science and Technology*, 57(48), 19497–19507. <https://doi.org/10.1021/acs.est.3c03609>
- 945 Renforth, P. (2012). The potential of enhanced weathering in the UK. *International Journal of Greenhouse Gas*  
946 *Control*, 10, 229–243. <https://doi.org/10.1016/j.ijggc.2012.06.011>
- 947 Renforth, Phil. (2019). The negative emission potential of alkaline materials. *Nature Communications*, 10(1).  
948 <https://doi.org/10.1038/s41467-019-09475-5>
- 949 Renforth, Phil., & Henderson, G. (2017). Assessing ocean alkalinity for carbon sequestration. *Reviews of*  
950 *Geophysics*, 55(3), 636–674. <https://doi.org/10.1002/2016RG000533>
- 951 Reynaert, S., Vienne, A., Boeck, H. J. De, Janssens, I., Portillo-estrada, M., Verbruggen, E., & Vicca, S. (2023).  
952 *Basalt addition improved climate change adaptation potential of young grassland monocultures under more*  
953 *persistent precipitation regimes*.
- 954 Rijnders, J., Vienne, A., & Vicca, S. (2024). *Effects of basalt , concrete fines , and steel slag on maize growth and*  
955 *heavy metal accumulation in an enhanced weathering experiment*. October, 1–34.
- 956 Rowley, M. C., Grand, S., & Verrecchia, É. P. (2018). Calcium-mediated stabilisation of soil organic carbon.  
957 *Biogeochemistry*, 137(1–2), 27–49. <https://doi.org/10.1007/s10533-017-0410-1>
- 958 Ryan, P. C., Hillier, S., & Wall, A. J. (2008). Stepwise effects of the BCR sequential chemical extraction procedure  
959 on dissolution and metal release from common ferromagnesian clay minerals: A combined solution chemistry  
960 and X-ray powder diffraction study. *Science of the Total Environment*, 407(1), 603–614.  
961 <https://doi.org/10.1016/j.scitotenv.2008.09.019>
- 962 Schindlbacher, A., Beck, K., Holzheu, S., & Borken, W. (2019). Inorganic Carbon Leaching From a Warmed and  
963 Irrigated Carbonate Forest Soil. *Frontiers in Forest and Global Change*, 2(August), 1–13.  
964 <https://doi.org/10.3389/ffgc.2019.00040>
- 965 Shamshuddin, J., Anda, M., Fauziah, C. I., & Omar, S. S. R. (2011). Growth of cocoa planted on highly weathered  
966 soil as affected by application of basalt and/or compost. *Communications in Soil Science and Plant Analysis*,  
967 42(22), 2751–2766. <https://doi.org/10.1080/00103624.2011.622822>
- 968 Smith, P., Davis, S. J., Creutzig, F., Fuss, S., Minx, J., Gabrielle, B., Kato, E., Jackson, R. B., Cowie, A., Kriegler,  
969 E., Van Vuuren, D. P., Rogelj, J., Ciais, P., Milne, J., Canadell, J. G., McCollum, D., Peters, G., Andrew, R.,  
970 Krey, V., ... Yongsung, C. (2016). Biophysical and economic limits to negative CO<sub>2</sub> emissions. *Nature Climate*  
971 *Change*, 6(1), 42–50. <https://doi.org/10.1038/nclimate2870>
- 972 Spanka, M. (2018). *Sequential extraction of chromium , molybdenum , and vanadium in basic oxygen furnace slags*.  
973 23082–23090.
- 974 Steinwider, L., Boito, L., Frings, P. J., Niron, H., Rijnders, J., de Schutter, A., Vienne, A., & Vicca, S. (2025).  
975 Beyond Inorganic C: Soil Organic C as a Key Pathway for Carbon Sequestration in Enhanced Weathering.  
976 *Global Change Biology*, 31(7). <https://doi.org/10.1111/gcb.70340>
- 977 Strefler, J., Amann, T., Bauer, N., Kriegler, E., & Hartmann, J. (2018). Potential and costs of carbon dioxide removal  
978 by enhanced weathering of rocks. *Environmental Research Letters*, 13(3). <https://doi.org/10.1088/1748-9326/aaa9c4>
- 980 Suarez, D. L., & Grieve, C. M. (1988). Predicting cation ratios in corn from saline solution composition. *Journal of*  
981 *Experimental Botany*, 39(5), 605–612. <https://doi.org/10.1093/jxb/39.5.605>
- 982 Swoboda, P., Döring, T. F., & Hamer, M. (2021). Remineralizing soils? The agricultural usage of silicate rock  
983 powders: A review. *Science of the Total Environment*, 807(150976), 18.  
984 <https://doi.org/10.1016/j.scitotenv.2021.150976>
- 985 Takaya, Y., Wu, M., & Kato, Y. (2019). Unique environmental conditions required for dawsonite formation:  
986 Implications from dawsonite synthesis experiments under alkaline conditions. *ACS Earth and Space*  
987 *Chemistry*, 3(2), 285–294. <https://doi.org/10.1021/acsearthspacechem.8b00121>
- 988 Taylor, L., Driscoll, C., Groffman, P., Rau, G., Blum, J., & Beerling, D. (2021). Increased carbon capture by a silicate-  
989 treated forested watershed affected by acid deposition. *Biogeosciences Discussions*, 1–29.  
990 <https://doi.org/10.5194/bg-2020-288>

- 991 te Pas, E. E. E. M., Hagens, M., & Comans, R. N. J. (2023). Assessment of the enhanced weathering potential of  
 992 different silicate minerals to improve soil quality and sequester CO<sub>2</sub>. *Frontiers in Climate*, 4.  
 993 <https://doi.org/10.3389/fclim.2022.954064>
- 994 Tessier, A., Campbell, P. G. C., & Bisson, M. (1979). Sequential Extraction Procedure for the Speciation of  
 995 Particulate Trace Metals. *Analytical Chemistry*, 51(7), 844–851. <https://doi.org/10.1021/ac50043a017>
- 996 Van Bemmelen, J. (1890). Über Die Bestimmung Des Wassers, Des Humus, Des Schwefels, Der in Den Colloïdalen  
 997 Silikaten Gebundenen Kieselsäure, Des Mangans U. S. W. Im Ackerboden. *Die Landwirthschaftlichen*  
 998 *Versuchs-Stationen*, 37, 279–290.
- 999 Van Straaten, P. (2006). Farming with rocks and minerals: Challenges and opportunities. *Anais Da Academia*  
 1000 *Brasileira de Ciencias*, 78(4), 731–747. <https://doi.org/10.1590/S0001-37652006000400009>
- 1001 Vienne, A., Frings, P., Poblador, S., Steinwidder, L., Rijnders, J., Schoelynck, J., Vinduskova, O., & Vicca, S. (2023).  
 1002 *Soil carbon sequestration and the role of earthworms in an Enhanced Weathering mesocosm experiment*.
- 1003 Vienne, A., Frings, P., Poblador, S., Steinwidder, L., Rijnders, J., Schoelynck, J., Vinduskova, O., & Vicca, S. (2024).  
 1004 Earthworms in an enhanced weathering mesocosm experiment : Effects on soil carbon sequestration , base  
 1005 cation exchange and soil CO<sub>2</sub> efflux. *Soil Biology and Biochemistry*, 199(June), 109596.  
 1006 <https://doi.org/10.1016/j.soilbio.2024.109596>
- 1007 Vienne, A., Poblador, S., Portillo-estrada, M., Hartmann, J., Ijehon, S., Wade, P., & Vicca, S. (2022). Enhanced  
 1008 Weathering Using Basalt Rock Powder : Carbon Sequestration , Co-benefits and Risks in a Mesocosm Study  
 1009 With *Solanum tuberosum*. *Frontiers in Climate*, 4(May), 1–14. <https://doi.org/10.3389/fclim.2022.869456>
- 1010 Wolf-Gladrow, D. A., Zeebe, R. E., Klaas, C., Körtzinger, A., & Dickson, A. G. (2007). Total alkalinity: The explicit  
 1011 conservative expression and its application to biogeochemical processes. *Marine Chemistry*, 106(1-2 SPEC.  
 1012 ISS.), 287–300. <https://doi.org/10.1016/j.marchem.2007.01.006>
- 1013 Xu, T., Yuan, Z., Vicca, S., Goll, D. S., Li, G., Lin, L., Chen, H., Bi, B., Chen, Q., Li, C., Wang, X., Wang, C., Hao,  
 1014 Z., Fang, Y., & Beerling, D. J. (2024). Enhanced silicate weathering accelerates forest carbon sequestration  
 1015 by stimulating the soil mineral carbon pump. *Global Change Biology*, 30(8), 1–17.  
 1016 <https://doi.org/10.1111/gcb.17464>
- 1017 Zhang, S., Planavsky, N. J., Katchinoff, J., Raymond, P. A., Kanzaki, Y., Reershemius, T., & Reinhard, C. T. (2022).  
 1018 River chemistry constraints on the carbon capture potential of surficial enhanced rock weathering. *Limnology*  
 1019 *and Oceanography*, 67(S2), S148–S157. <https://doi.org/10.1002/lno.12244>

1020